Optimized Synthesis and Indium complex formation with the bifunctional chelator NODIA-Me

Christian Weinmann[2,5], Jason P. Holland[4], Tilman Läppchen[2,3], Harald Scherer[5], Stephan Maus[1], Tobias Stemler[1], Hendrik Bohnenberger[1], Samer Ezziddin[1], Philipp Kurz[5*] and Mark D. Bartholomä[1,2*]

[1] Department of Nuclear Medicine, University Hospital Saarland, Saarland University, Kirrbergerstrasse, D-66421, Homburg, Germany

[2] Department of Nuclear Medicine, University Hospital Freiburg, D-79106, Freiburg, Germany

[3] Department of Nuclear Medicine, Inselspital, Bern University Hospital and University of Bern, Freiburgstrasse, CH-3010 Bern, Switzerland

[4] Department of Chemistry, University of Zurich, Winterthurerstrasse 190, CH-8057, Zurich, Switzerland

[5] Institute for Inorganic and Analytical Chemistry, Albert-Ludwigs-University Freiburg, Albertstrasse 21, D-79104, Freiburg, Germany

*** Corresponding Authors:**

Dr. Mark D. Bartholomä

E-mail: mark.bartholomae@uks.eu

Prof. Dr. Philipp Kurz

E-mail: philipp.kurz@ac.uni-freiburg.de

Content

Syntheses

*2-Bromo-N-ethylacetamide (**9**)*

2-Bromo-*N*-ethylacetamide was prepared according to the literature with minor modifications.[14] Briefly, to ethylamine (66-72% in H_2O, 3 mL) and CH_2Cl_2 (17 mL) potassium carbonate (2 M, 18 mL) at 5 °C was added dropwise bromoacetylbromide (2.2 mL, 25.33 mmol) in CH_2Cl_2 (17 mL). After 30 min, cooling was removed and the solution stirred for additional 17 h. The aqueous phase was separated and extracted two times with CH_2Cl_2 (2 x 5 mL). The combined organic layers were washed with H_2O (2 x 10 mL) and dried using sodium sulfate. After removal of the solvent, the product was obtained as a colorless, hygroscopic solid (2.51 g, 61%). ^{1}H-NMR (300 MHz, $CDCl_3$) δ = 6.52 (br, 1H, NH), 3.86 (s, 2H, Br-CH_2), 3.32 (dq, J = 7.3, 5.7 Hz, 2H, ethyl-CH_2), 1.17 (t, J = 7.3 Hz, 3H, ethyl-CH_3) ppm. ^{13}C-NMR (75 MHz, $CDCl_3$) δ = 165.3 (carbonyl), 35.2 (ethyl-CH_2), 29.4 (Br-CH_2), 14.6 (ethyl-CH_3) ppm. HR-ESI-MS calcd m/z for $C_4H_9BrNO^+$: 167.9842, found: 167.9842. IR (ATR) ν = 3270 (m), 3089 (w), 2976 (w), 2934 (w), 2874 (w), 1643 (s), 1557 (s), 1434 (m), 1377 (w), 1359 (w), 1317 (m), 1210 (m), 1153 (m), 1097 (w), 1061 (w), 941 (w), 919 (w), 709 (m), 654 (m), 547 (m) cm^{-1}.

*Di-tert-butyl 7-(2-(ethylamino)-2-oxoethyl)-1,4,7-triazanonane-1,4-dicarboxylate (**10**)*

Under argon, compound **5** (2.96 g, 8.98 mmol) and potassium carbonate (5 g, 36.24 mmol) were added to dry acetonitrile (70 mL). Compound **9** (1.5 g, 8.98 mmol) in dry acetonitrile (20 mL) was added dropwise and the reaction was refluxed for 18 h. The solvent was removed and the residue dissolved in saturated $NaHCO_3$ solution (50 mL) followed by extraction with chloroform (3 x 15 mL). The combined organic layers were dried using sodium sulfate and after removal of the solvent, the crude product was purified by silica gel column chromatography (ethyl acetate) to give compound **10** as an orange oil (3.31 g, 89%) containing one main isomer and two minor isomers. ^{1}H and ^{13}H NMR data are provided in tabular form in the Supporting Information. ^{15}N-NMR (30 MHz, $CDCl_3$) δ = -294 (macrocycle-BOC), -263 (amide) ppm. HR-ESI-MS calcd m/z for $C_{20}H_{38}N_4O_5Na^+$: 437.2734, found: 437.2739. IR (ATR) ν = 3328 (w), 2973 (w), 2932 (w), 1677 (s), 1529 (w), 1463 (m), 1412 (m), 1365 (m), 1303 (w), 1244 (m), 1153 (s), 1138 (s), 1099 (m), 1035 (w), 998 (w), 972 (w), 857 (w), 772 (m), 752 (s), 665 (w) cm^{-1}. R_f value (silica gel): 0.66 (EA).

*N-ethyl-2-(1,4,7-triazanonan-1-yl)acetamide (**11**)*

Compound **10** (3.20 g, 7.72 mmol) was dissolved in CH_2Cl_2 (6 mL) and cooled to 0 °C. Trifluoroacetic acid (6 mL) was added dropwise and the reaction mixture was stirred for 2 h at r.t. The solvent was removed and the yellow solid residue was dissolved in H_2O (30 mL). The pH was adjusted to pH > 10 with sodium hydroxide solution and the aqueous phase was extracted with chloroform (5 mL) until the organic layer was colorless. The combined organic layers were dried using sodium sulfate and after removal of the solvent compound **11** was obtained as yellow oil (1.20 g, 73%). ^{1}H-NMR (300 MHz, $CDCl_3$) δ = 9.05 (br, 1H, amide-NH), 3.29 (dq, J = 7.3, 5.6 Hz, 2H, ethyl-CH_2), 3.25 (s, 2H, CH_2-bridge), 2.82 (s, 4H, macrocycle), 2.74 (m, 4H, macrocycle), 2.65 (m, 4H, macrocycle), 2.13 (br, 2H, macrocycle-NH), 1.14 (t, J = 7.3 Hz, 3H, ethyl-CH_3) ppm. ^{13}C-NMR (50 MHz, $CDCl_3$) δ = 172.5 (carbonyl), 60.7 (CH_2-bridge), 54.5 (macrocycle), 48.1 (macrocycle), 46.7 (macrocycle), 33.9 (ethyl-CH_2), 14.9 (ethyl-CH_3) ppm. HR-ESI-MS calcd m/z for $C_{10}H_{23}N_4O^+$: 215.1866, found: 215.1861. IR

(ATR) ν = 3318 (w), 2970 (w), 2909 (w), 2814 (w), 1648 (s), 1539 (m), 1452 (m), 1354 (m), 1295 (m), 1257 (m), 1140 (m), 1072 (w), 1036 (w), 978 (w), 900 (w), 747 (s), 662 (m) cm^{-1}.

*2-(4,7-Bis((1-methyl-1H-imidazol-2-yl)methyl)-1,4,7-triazanonan-1-yl)-N-ethylacetamide NODIA-Me-NH-Et (**12**)*

Under argon, compound **11** (0.84 g, 3.93 mmol), 1-methyl-2-imidazolecarboxaldehyde (1.36 g, 12.36 mmol) were dissolved in dry THF (20 mL) and the mixture was stirred for 3 h at r.t. Next, sodium triacetoxyborohydride (0.85 g, 4.03 mmol) was added in small portions and stirring was continued for additional 17 h. More sodium triacetoxyborohydride (3 x 0.85 g) was added in 1 h time intervals and the mixture was stirred for another 2 h. Then, H_2O (10 mL) was added, the pH was carefully adjusted to pH < 2 using TFA and stirring was continued for 30 min. The solvents were removed and the residue was purified using automated flash chromatography to give NODIA-Me-NH-Et (**12**) · 3 TFA · 2 H_2O as yellow resin (1.19 g, 62%). ^{1}H-NMR (300 MHz, D_2O, pD < 2) δ = 7.46 (d, J = 2.1 Hz, 2H, imidazole), 7.45 (d, J = 2.1 Hz, 2H, imidazole), 4.24 (d, J = 15.9 Hz, 2H, CH_2-bridge imidazole), 4.17 (s, 2H, CH_2-bridge peptide), 4.15 (d, J = 15.9 Hz, 2H, CH_2-bridge imidazole), 3.85 (s, 6H, imidazole-Me), 3.48, 3.35 (m, 4H, macrocycle), 3.33 (q, J = 7.3 Hz, 2H, ethyl-CH_2), 3.15, 2.99 (m, 4H, macrocycle), 2.90, 2.54 (m, 4H, macrocycle), 1.15 (t, J = 7.3 Hz, 3H, ethyl-CH_3) ppm. ^{13}C-NMR (50 MHz, D_2O, pD < 2) δ = 164.7 (carbonyl), 142.9 (imidazole), 124.1 (imidazole), 118.7 (imidazole), 56.5 (CH_2-bridge peptide), 52.5 (macrocycle), 49.8 (macrocycle), 48.1 (CH_2-bridge imidazole), 45.9 (macrocycle), 35.0 (ethyl-CH_2), 34.4 (imidazole-Me), 13.2 (ethyl-CH_3) ppm. ^{14}N-NMR (22 MHz, D_2O, pD < 2) δ = -350 (macrocycle), -205 – -210 (imidazole) ppm. ^{15}N-NMR (30 MHz, D_2O, pD < 2) δ = -252 (peptide), -209 (imidazol-Me) ppm. HR-ESI-MS (ESI) calcd m/z for $C_{20}H_{35}N_8O^+$: 403.2928, found: 403.2929. IR (ATR) ν = 3088 (w), 2881 (w), 1738 (w), 1666 (s), 1605 (w), 1532 (w), 1497 (w), 1459 (w), 1405 (w), 1278 (w), 1174 (s), 1122 (s), 974 (m), 939 (m), 827 (m), 797 (s), 755 (m), 718 (s), 706 (s), 654 (m), 593 (m) cm^{-1}. Elemental analysis: calc. C: 40.00%, H: 5.29%, N: 14.35%, found C: 41.16%, H: 4.90%, N: 14.24%.

Syntheses of Metal Complexes

*Synthesis of [^{nat}In(NODIA-Me-NH-Et)] (In-**12**)*

Compound **12** (100 mg, 0.12 mmol) and indium(III)nitrate hydrate (63 mg, 0.2 mmol) were mixed in ammonium acetate buffer (0.1 M, pH 5.5, 2 mL) and heated for 15 min at 95 °C. The metal complex In-**12** was obtained after purification by automated flash chromatography and lyophilization as colorless resin (86 mg, 97%). ^{1}H-NMR (300 MHz, D_2O, pD < 2) δ = 7.24 (d, J = 1.6 Hz, 2H, imidazole), 7.15 (d, J = 1.6 Hz, 2H, imidazole), 4.47 (d, J = 16.4 Hz, 2H, CH_2-bridge imidazole), 4.31 (d, J = 16.4 Hz, 2H, CH_2-bridge imidazole), 3.88 (s, 2H, CH_2-bridge peptide), 3.66 (s, 6H, imidazole-Me), 3.39 (q, J = 7.3 Hz, 2H, ethyl-CH_2), 3.36 (m, 2H, macrocycle), 3.32 (m, 2H, macrocycle), 3.32 (m, 2H, macrocycle), 3.25 (m, 2H, macrocycle), 3.12 (m, 2H, macrocycle), 3.00 (m, 2H, macrocycle), 1.12 (t, J = 7.3 Hz, 3H, ethyl-CH_3) ppm. ^{13}C-NMR (101 MHz, D_2O, pD < 2) δ = 170.0 (carbonyl), 144.0 (imidazole), 124.4 (imidazole), 124.1 (imidazole), 59.4 (CH_2-bridge peptide), 53.2 (CH_2-bridge imidazole), 52.1 (macrocycle), 51.1 (macrocycle), 51.5 (macrocycle), 35.6 (ethyl-CH_2), 32.3 (imidazole-Me), 13.0 (ethyl-CH_3) ppm. ^{15}N-NMR (41 MHz, D_2O, pD < 2) δ = -352 (macrocycles-peptide), -350 (macrocycle-imidazole), -249 (peptide), -218 (imidazol-Me), -167 (imidazole) ppm. HR-ESI-MS (ESI) calcd m/z for $C_{20}H_{32}InN_8O^+$: 515.1732, found: 515.1730. IR (ATR) ν = 3250 (w), 3133 (w), 2947

(w), 2883 (w), 1778 (w), 1737 (w), 1686 (m), 1640 (m), 1554 (w), 1513 (w), 1464 (w), 1426 (w), 1362 (w), 1304 (w), 1285 (w), 1189 (s), 1128 (s), 1022 (m), 986 (m), 912 (m), 884 (m), 849 (m), 815 (m), 796 (s), 761 (m), 728 (m), 717 (m), 705 (s), 676 (m), 659 (m), 602 (m) cm^{-1}. Elemental analysis: calc. C: 36.46%, H: 4.00%, N: 13.08%, found C: 34.45%, H: 3.97%, N: 12.36%.

*Synthesis of [^{nat}In(NODIA-Me-NaI-Ahx-PSMA)] (In-**13**)*

The bioconjugate **13** (500 µg, 0.51 µmol) dissolved in 250 µL H_2O was mixed with 250 µL of an indium chloride stock solution (1.5 equivalents) and heated at 95 °C for 15 min. After cooling to r.t., the conjugate In-**13** was purified using a C_{18} Sep Pak Light cartridge, which was preconditioned sequentially with EtOH and H_2O (each 5 mL). After loading, the cartridge was washed with 2 mL H_2O and the product was eluted using 1 mL EtOH:H_2O (50:50 v/v). Samples were then lyophilized to give In-**13** as colorless powder (492 mg, 0.45 µmol, 88%). RP-HPLC (analytical, UV: 220 nm): t_R (In-**13**) = 17:37 min. HR-ESI-MS calcd m/z for $C_{49}H_{68}N_{12}O_{10}In^+$: 1099.4215, found: 1099.4208.

NMR data

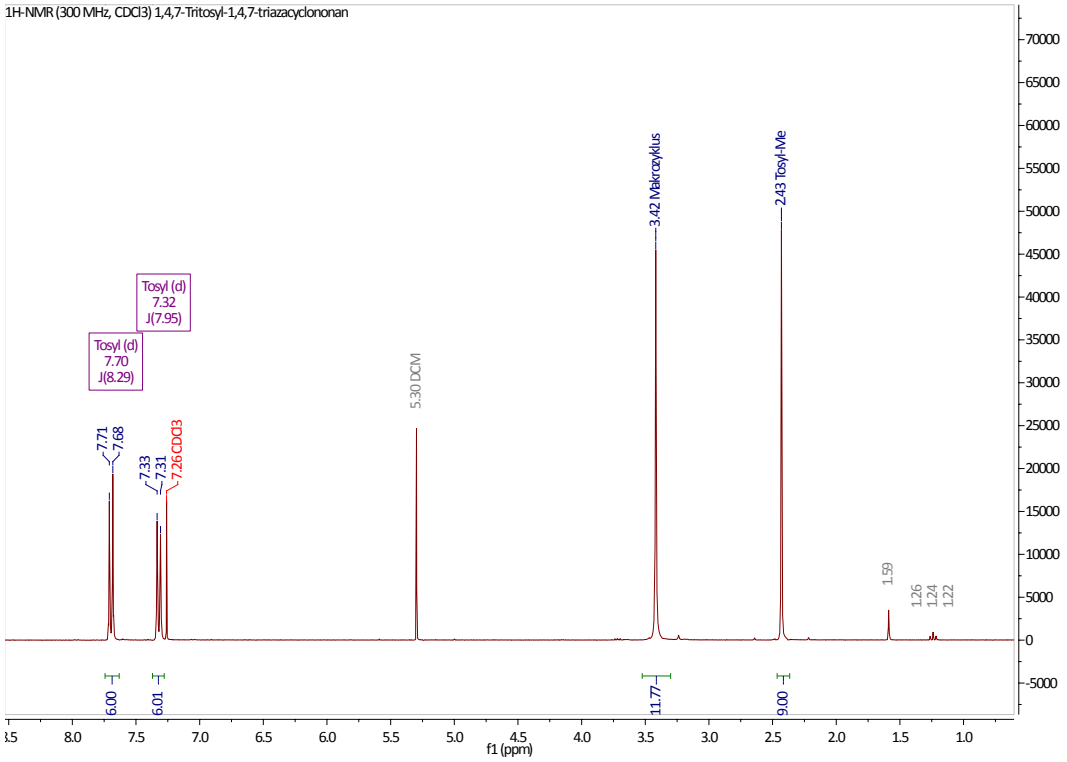

Figure S1. Proton NMR of **1**

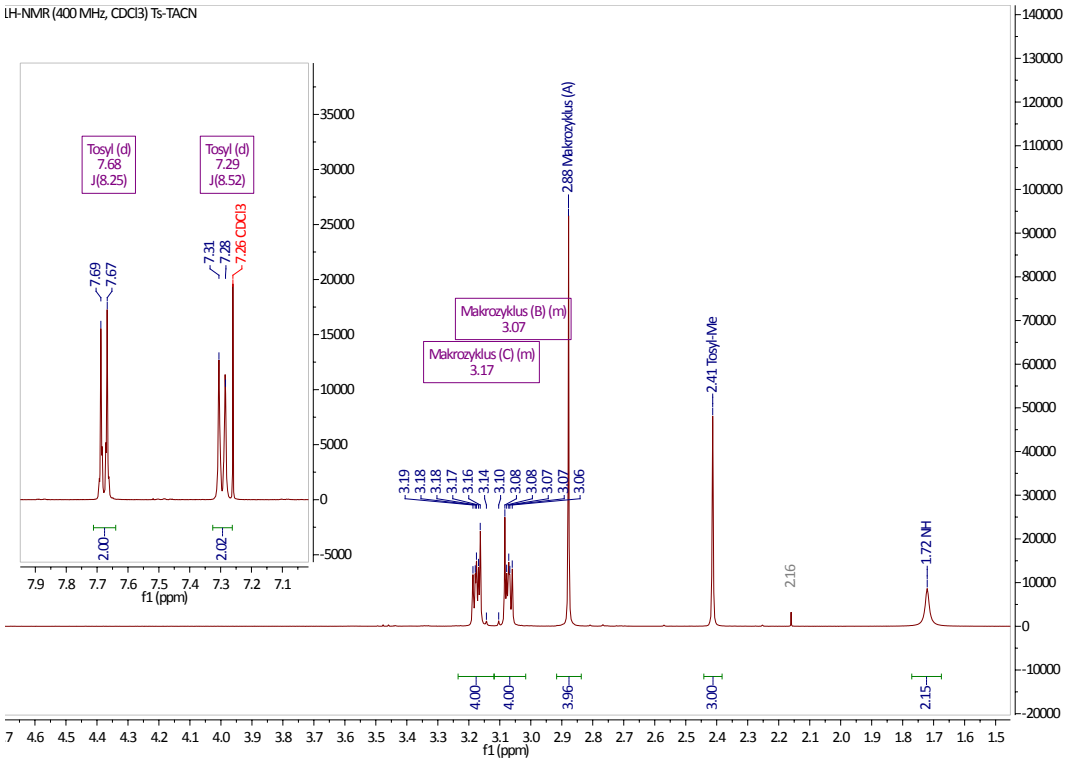

Figure S2. Proton NMR of **2**

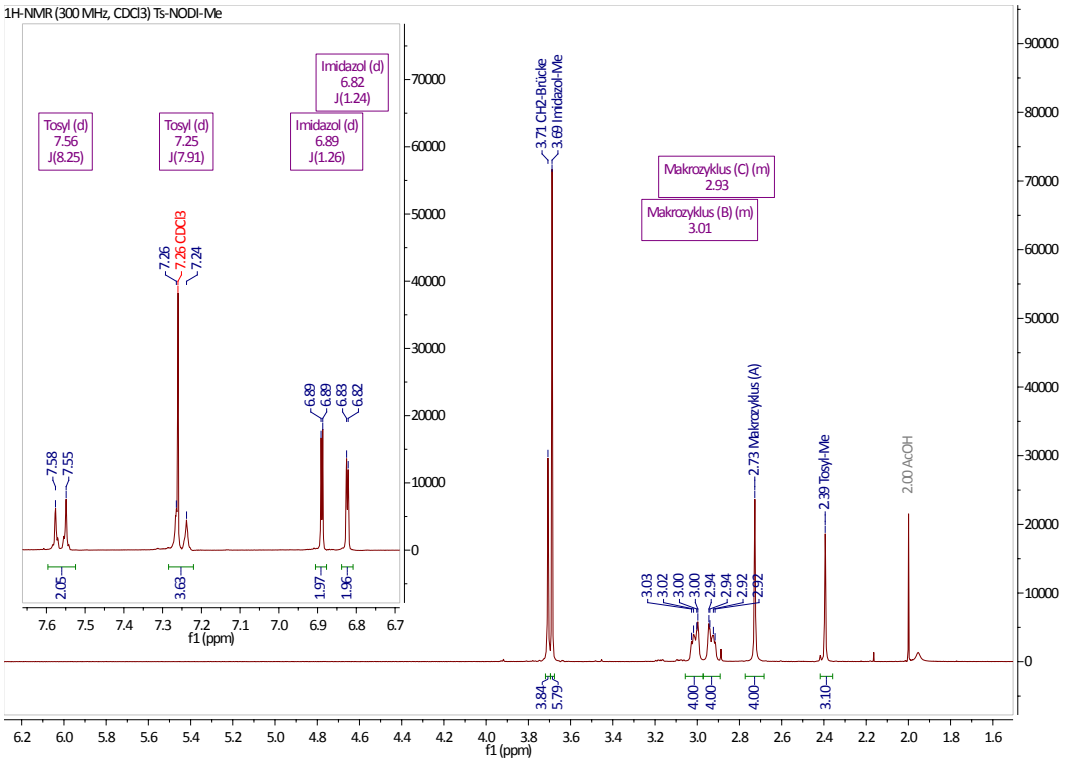

Figure S3. Proton NMR of **3**

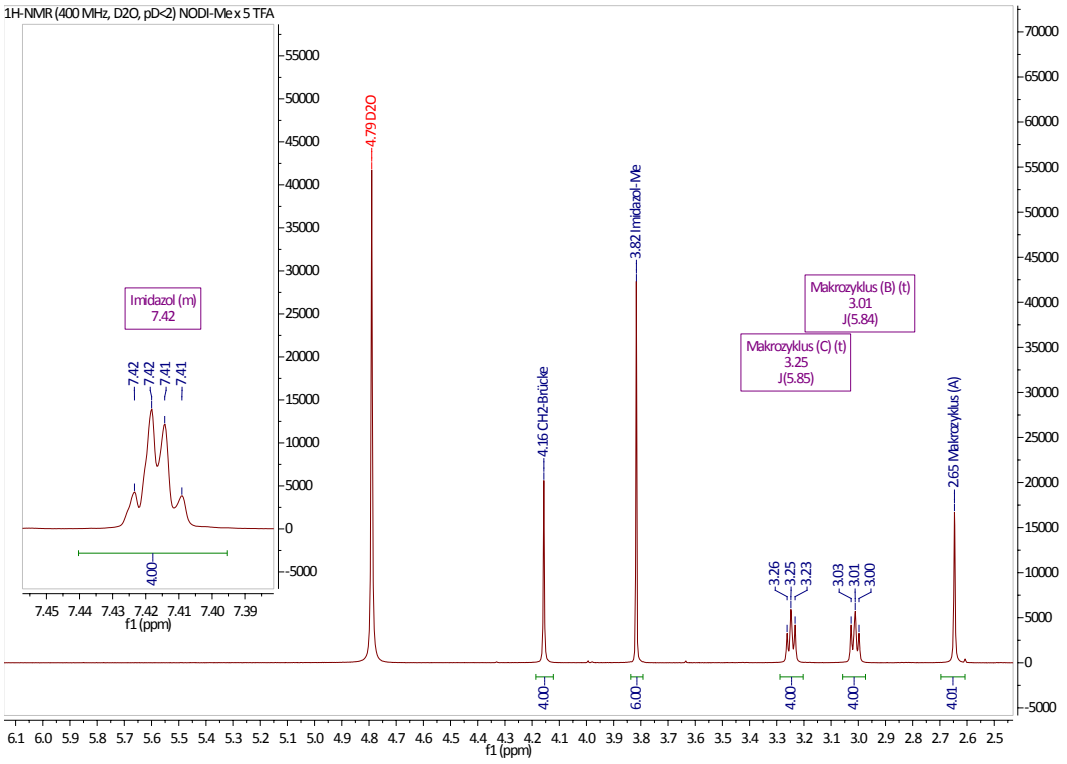

Figure S4. Proton NMR of **4**

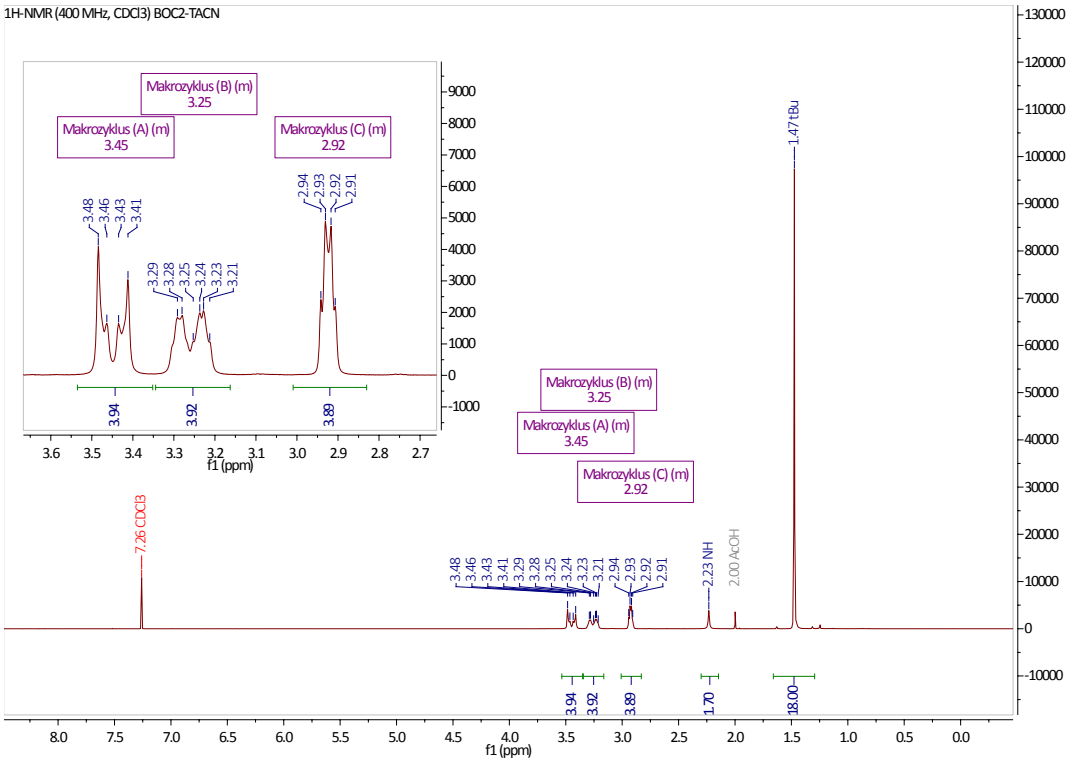

Figure S5. Proton NMR of **5**

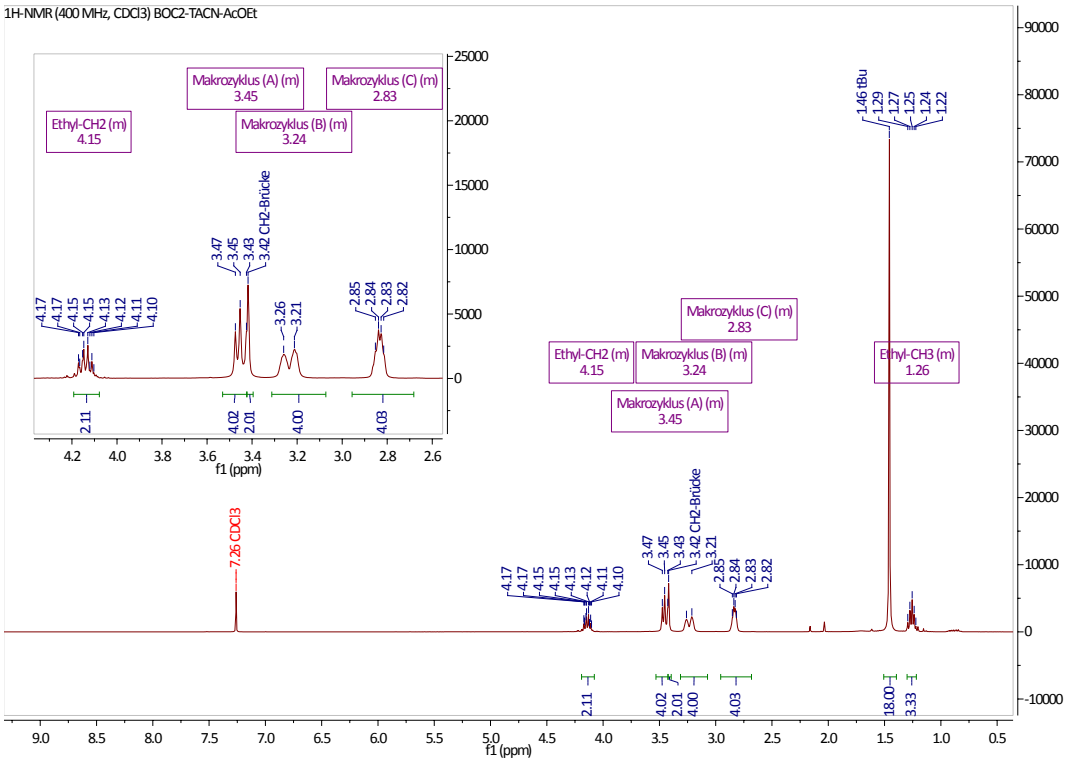

Figure S6. Proton NMR of **6**

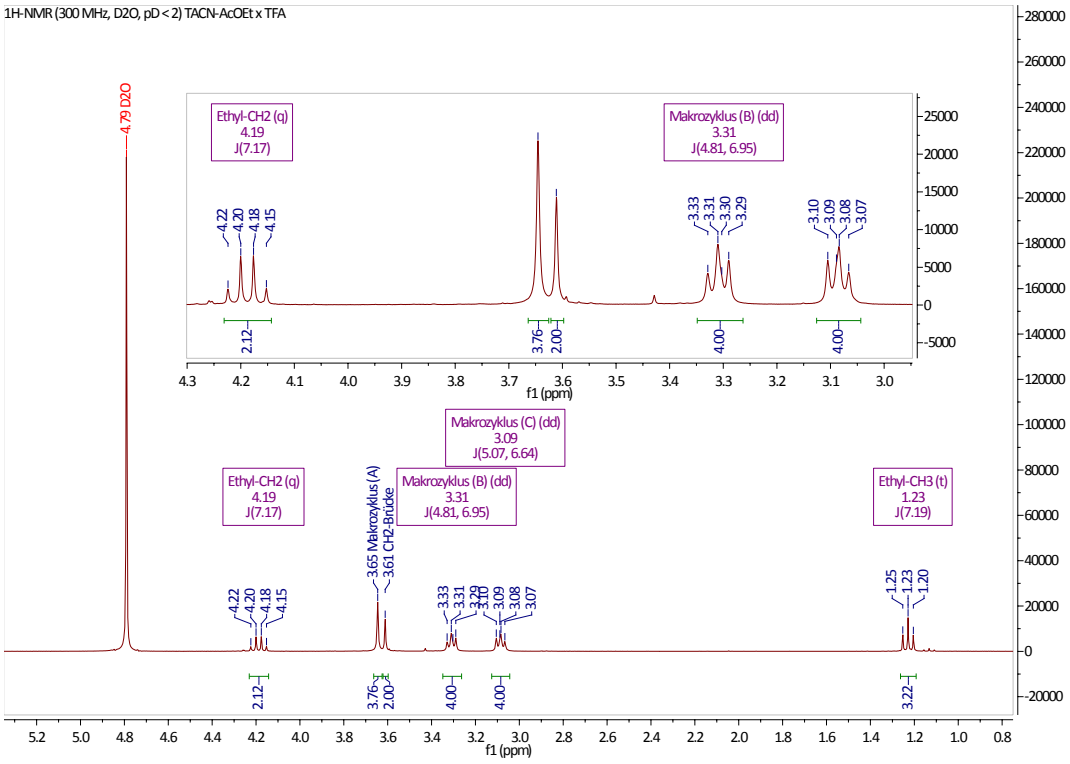

Figure S7. Proton NMR of **7**

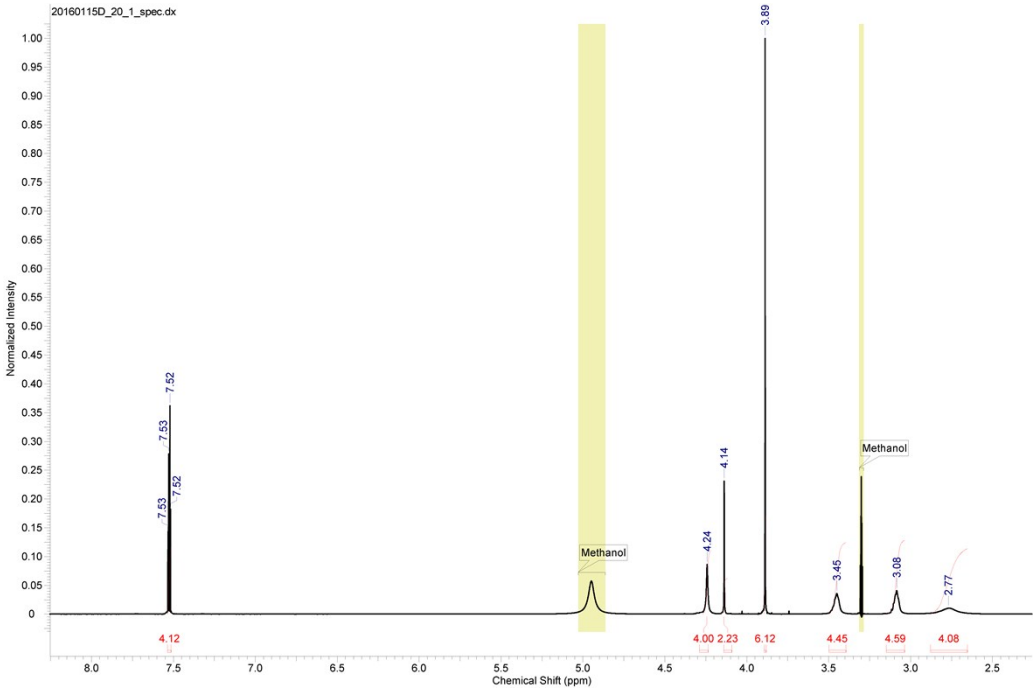

Figure S8. Proton NMR of **8**

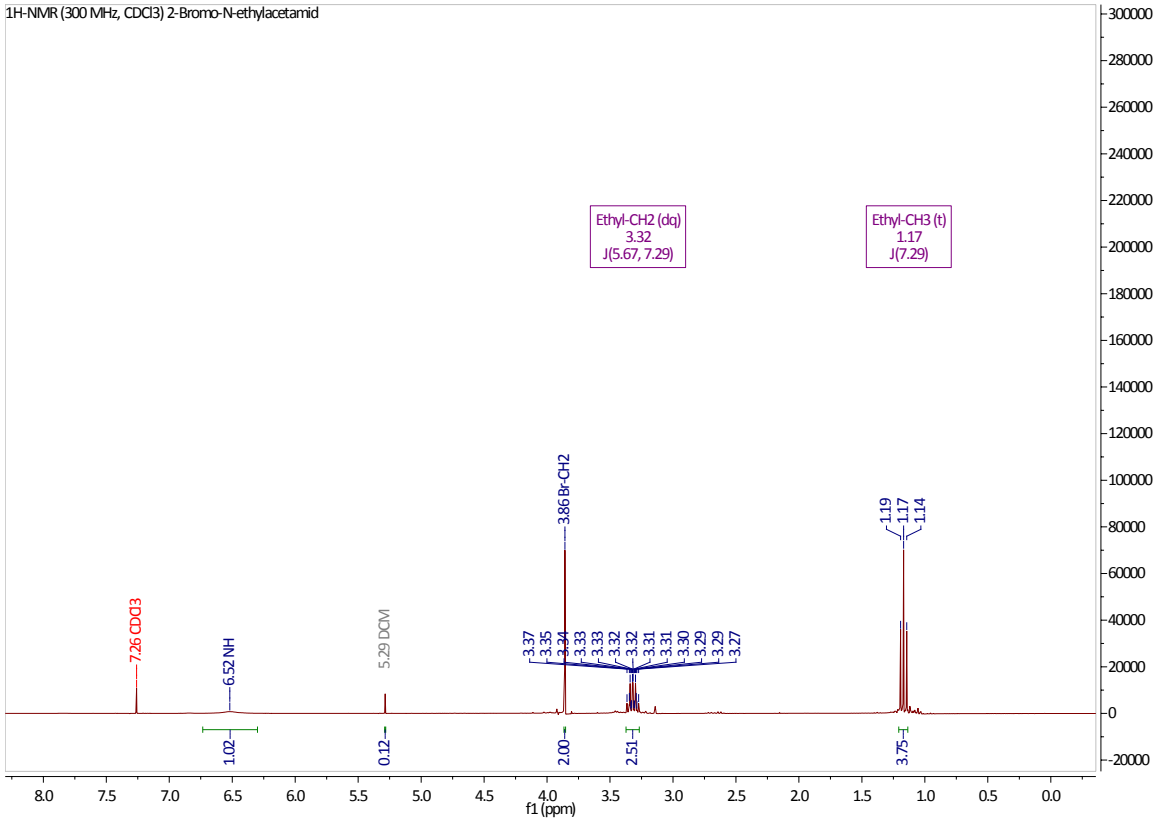

Figure S9. Proton NMR of **9**

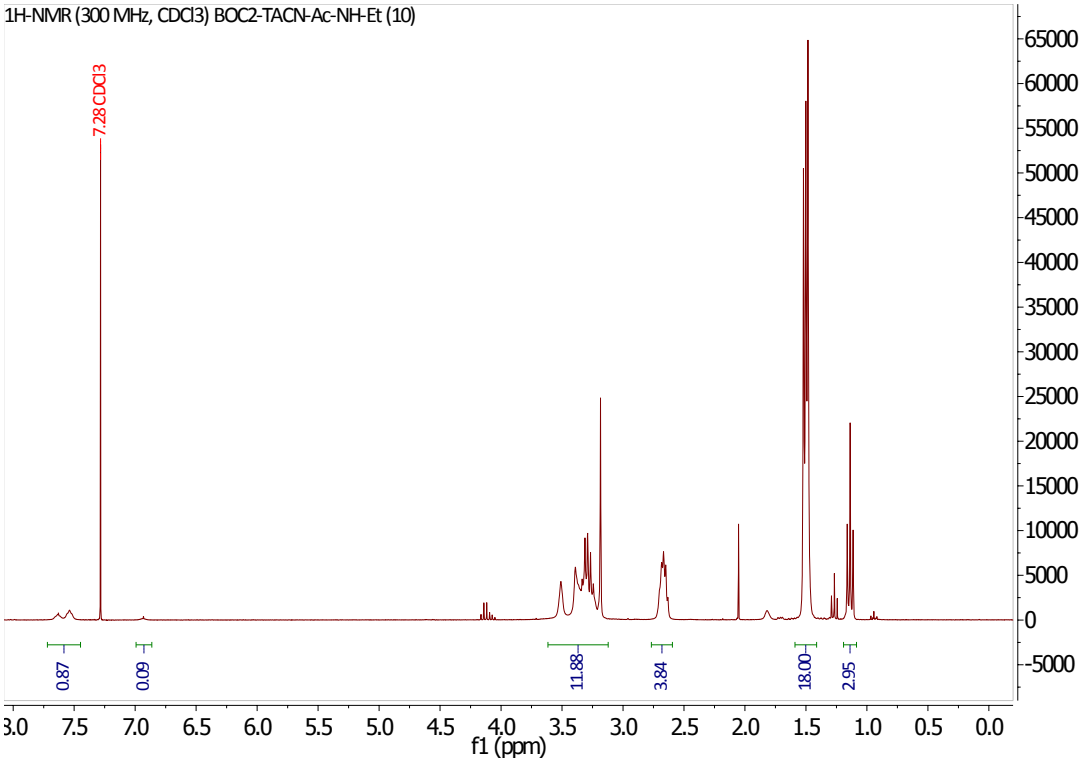

Figure S10. Proton NMR of **10**

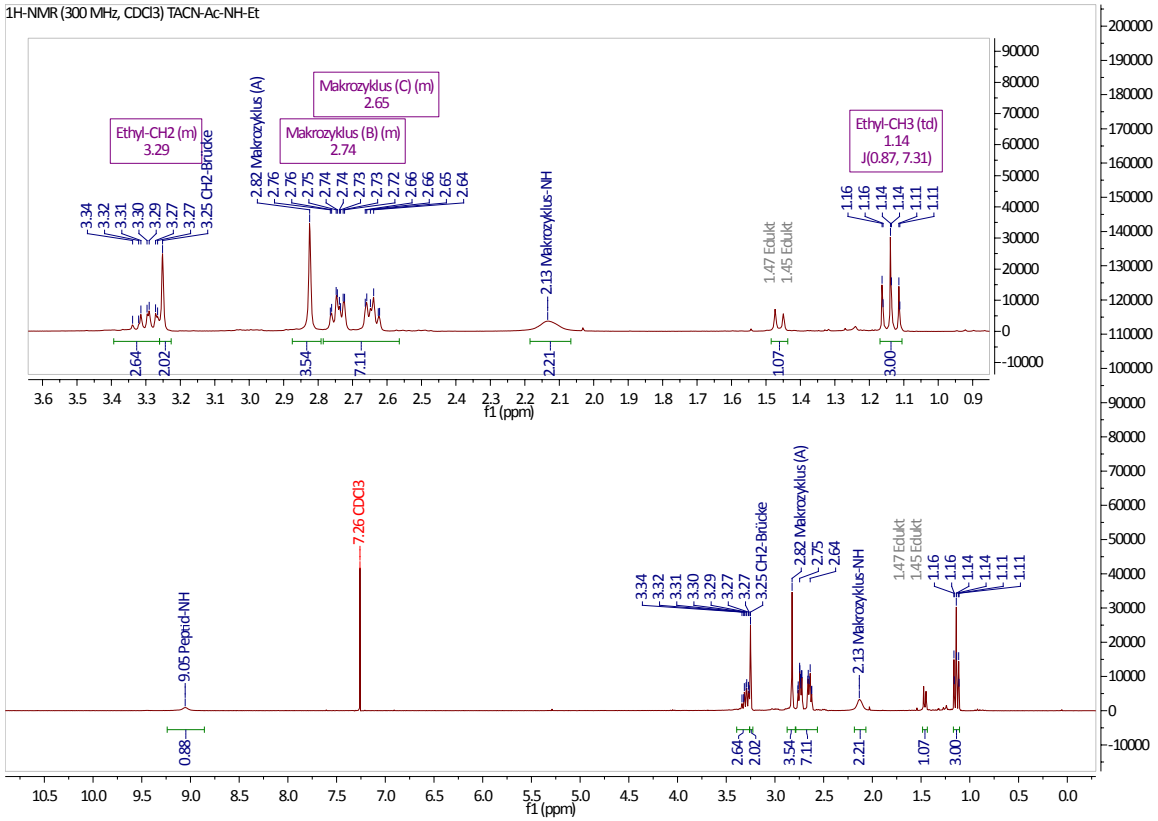

Figure S11. Proton NMR of **11**

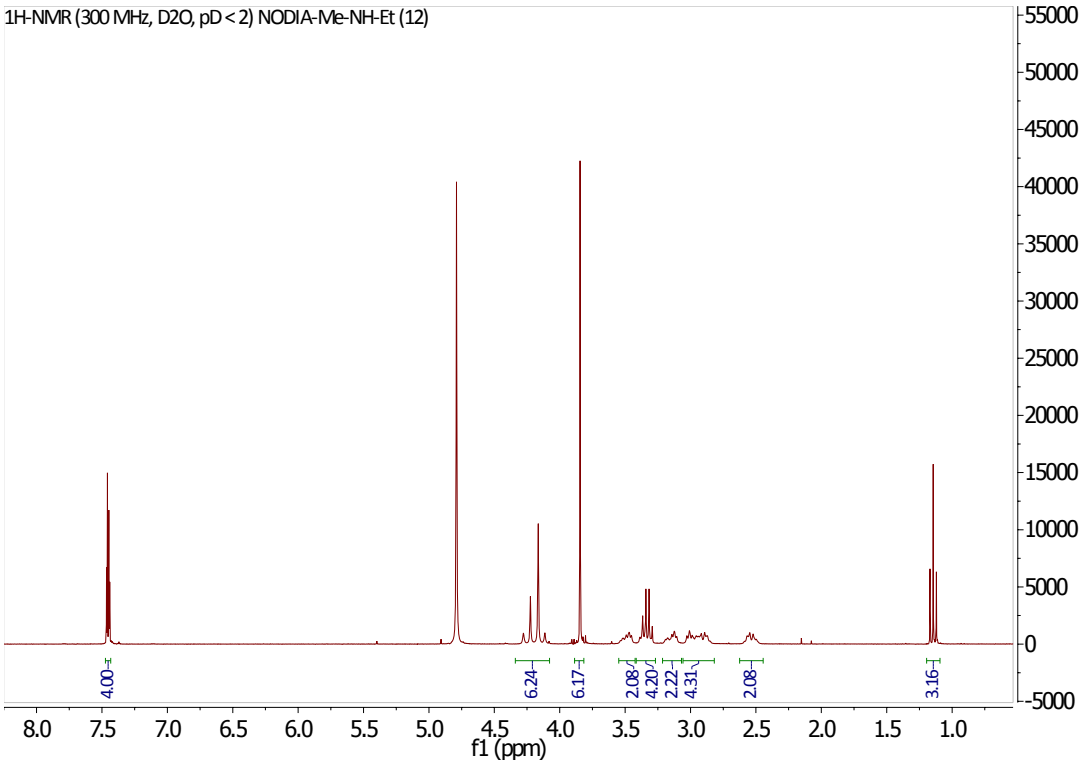

Figure S12. Proton NMR of **12**

Table S1. Assignment of proton and carbon NMR signals of **10**. Signals of the main isomer are underlined. Chemical shifts are given in ppm relative to TMS.

	δ ^{13}C (75 MHz, $CDCl_3$)	δ ^{1}H (300 MHz, $CDCl_3$)
peptide-NH	-	7.61, <u>7.51</u>, 6.91
Ac-NH-Et-carbonyl	<u>171.3</u> (br), 171.2 (br)	-
BOC-carbonyl	156.6, 155.9 (br), 155.8	-
tBu	<u>80.2</u>, 79.9, 79.8 (br)	-
CH_2 (acetic acid)	<u>63.3</u> (br), 62.8	3.14 (br, 2H)
macrocycle C	54.8	2.61 (br, 4H)
	<u>53.9, 53.8</u>	<u>2.63</u>
macrocycle B	53.6	3.20 (br, 4H)
	<u>51.4</u>	<u>3.26</u>
	<u>50.2</u>	<u>3.27</u>
	48.2	3.28
macrocycle A	50.7	3.47 (br, 4H)
	50.1	3.35
	49.7	3.47
	48.9	3.33
ethyl-CH_2	33.8 (br)	3.26 (q, *J*=7.2Hz, 2H)
	33.8 (br)	3.23 (q, *J*=7.2Hz, 2H)
ethyl-CH_3	15.1 (br)	1.10 (t, *J*=7.2Hz, 3H)

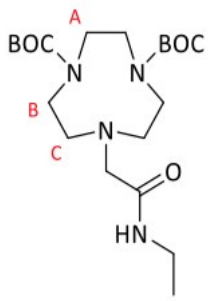

Table S2. Assignment of proton and carbon NMR signals of **12** and In-**12** in D_2O (pD < 2). Chemical shifts are given in ppm relative to TMS.

Signal	metal-free **12**		In-**12**	
	δ^{13}C (50 MHz)	δ^{1}H (300 MHz)	δ^{13}C (101 MHz)	δ^{1}H (300 MHz)
carbonyl	164.7	-	170.0	-
imidazole-2	142.9	-	144.0	-
imidazole-5	124.1	7.46	124.1	7.24
imidazole-4	118.7	7.45	124.4	7.15
CH_2 amide	56.5	4.17	59.4	3.88
macrocycle C	52.5	3.48	52.1	3.32
		3.35		3.00
macrocycle A	49.8	2.90	51.1	3.36
		2.54		3.25
CH_2 imidazole	48.1	4.24	53.2	4.47
		4.15		4.31
macrocycle B	45.9	3.15	51.5	3.32
		2.99		3.12
ethyl-CH_2	35.0	3.33	35.6	3.39
imidazole-CH_3	34.4	3.85	32.3	3.66
ethyl-CH_3	13.2	1.15	13.0	1.12

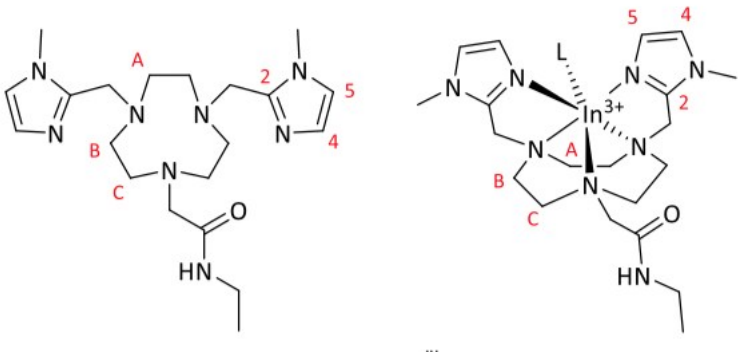

MS spectrometry

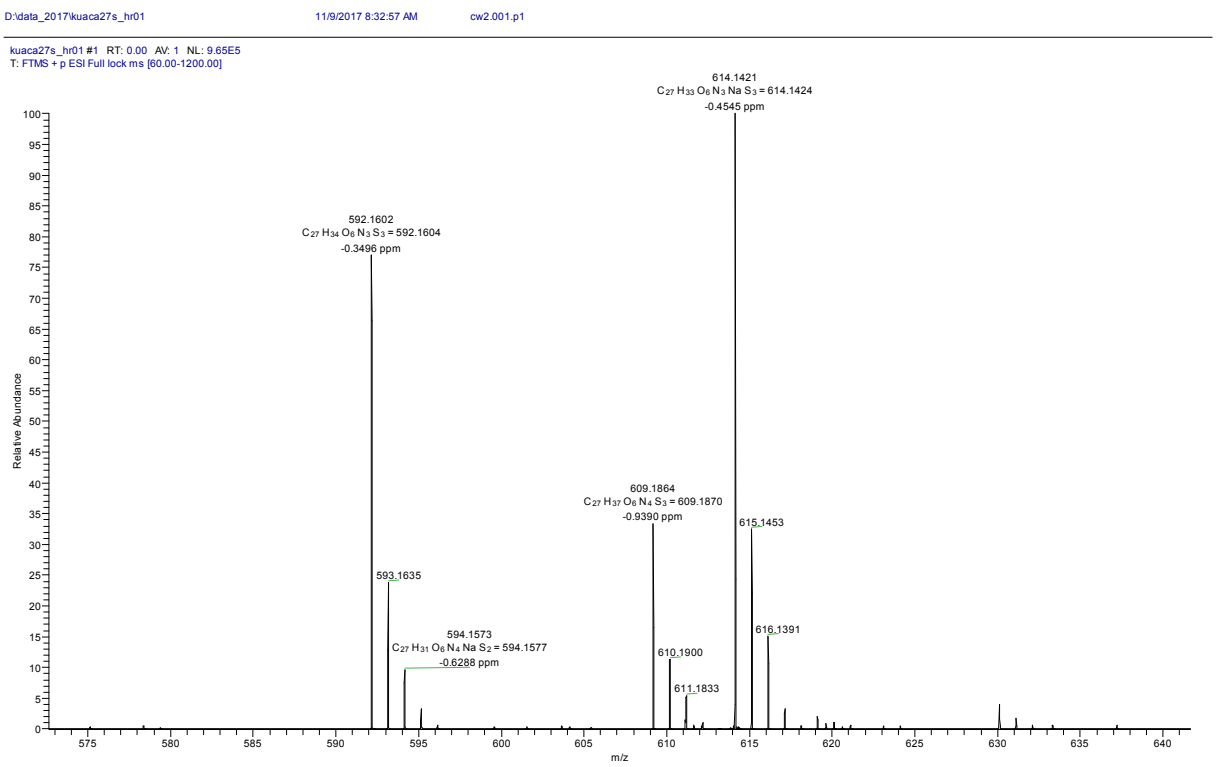

Figure S13. HR-ESI(+) spectrum of 1,4,7-tritosyl-1,4,7-triazonane (**1**)

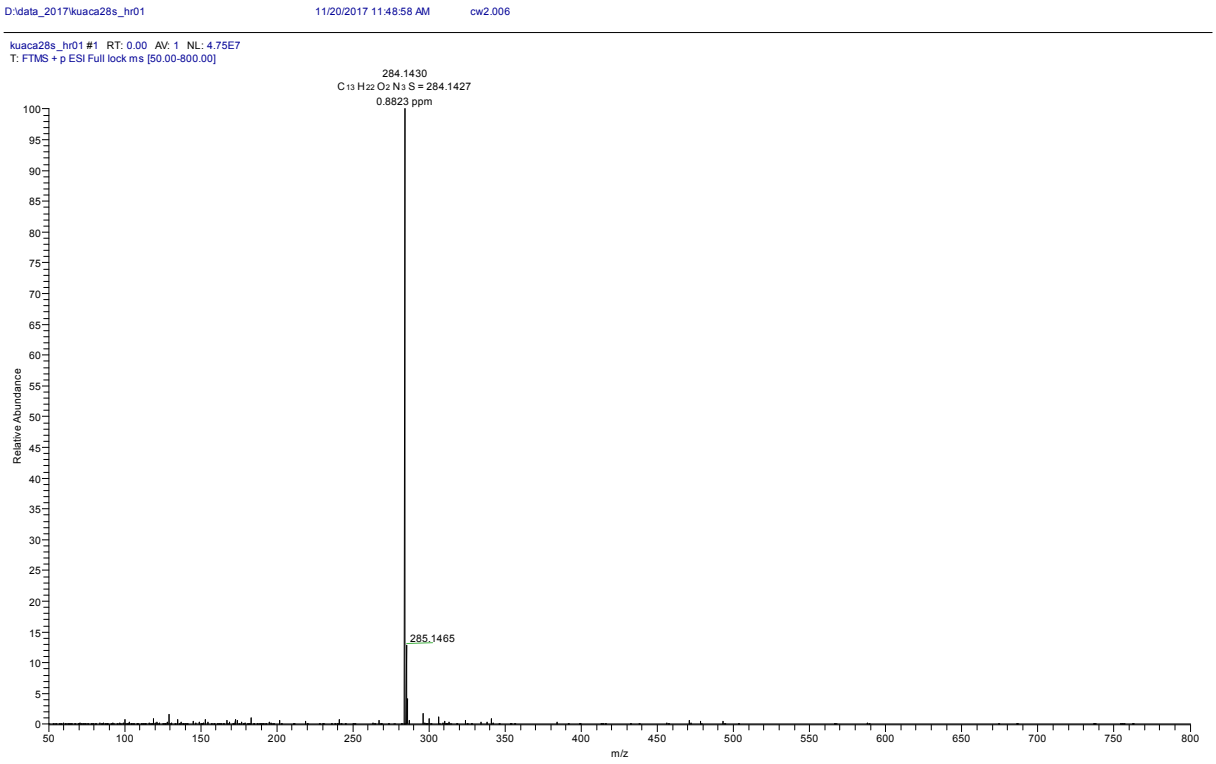

Figure S14. HR-ESI(+) spectrum of 1-tosyl-1,4,7-triazonane (**2**)

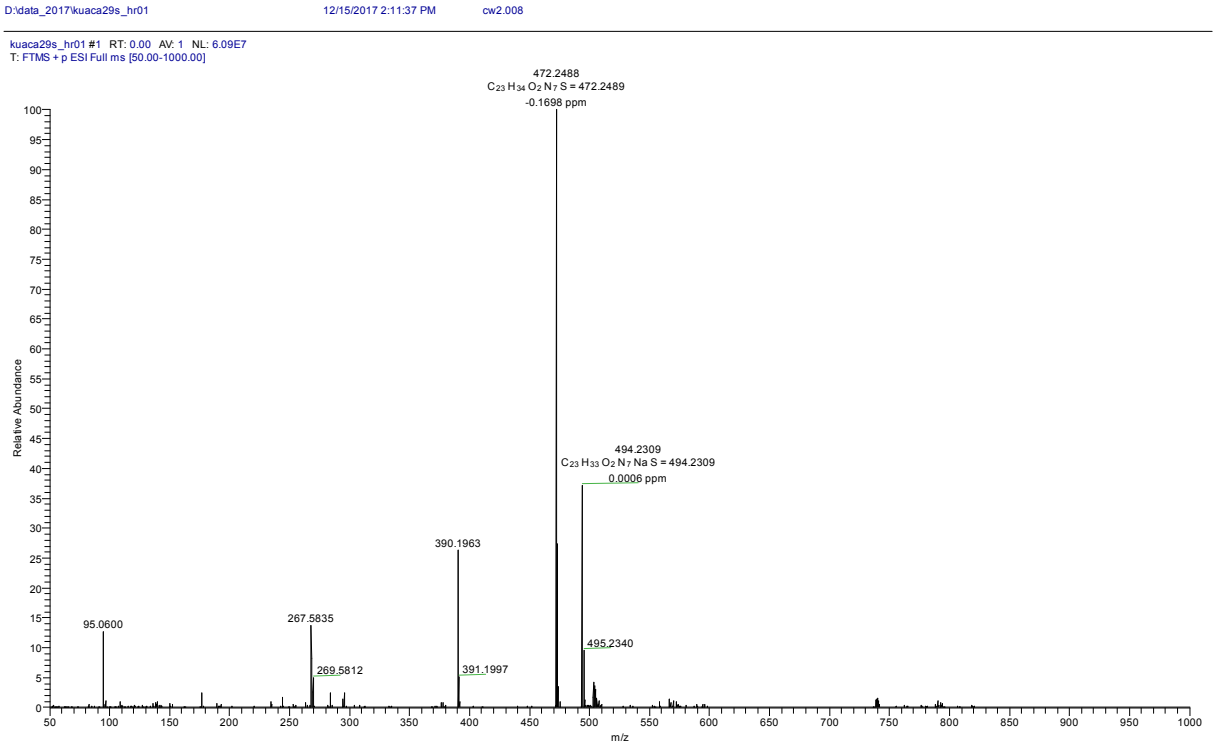

Figure S15. HR-ESI(+) spectrum of 1-((1-methyl-1H-imidazol-2-yl)methyl)-4-((1-methyl-4,5-dihydro-1H-imidazol-2-yl)methyl)-7-tosyl-1,4,7-triazonane (**3**)

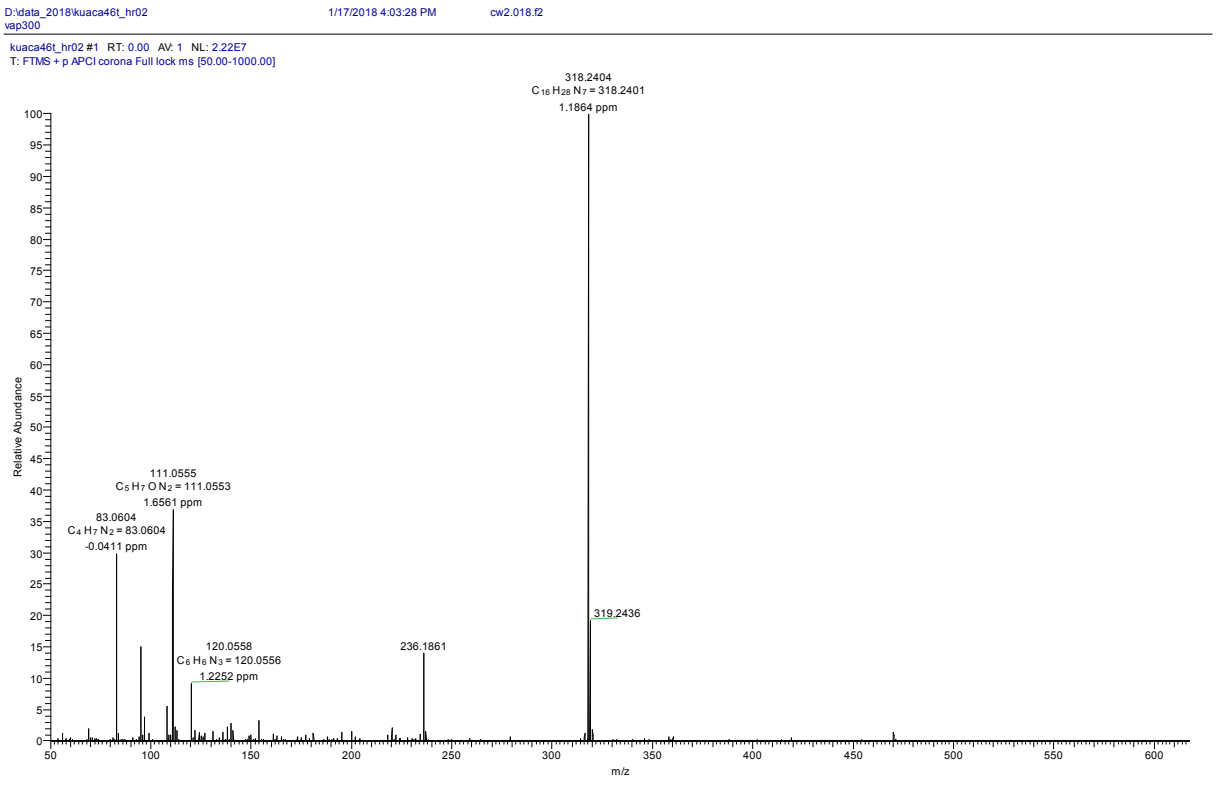

Figure S16. HR-ESI(+) spectrum of 1-((1-methyl-1H-imidazol-2-yl)methyl)-4-((1-methyl-4,5-dihydro-1H-imidazol-2-yl)methyl)-1,4,7-triazonane NODI-Me (**4**)

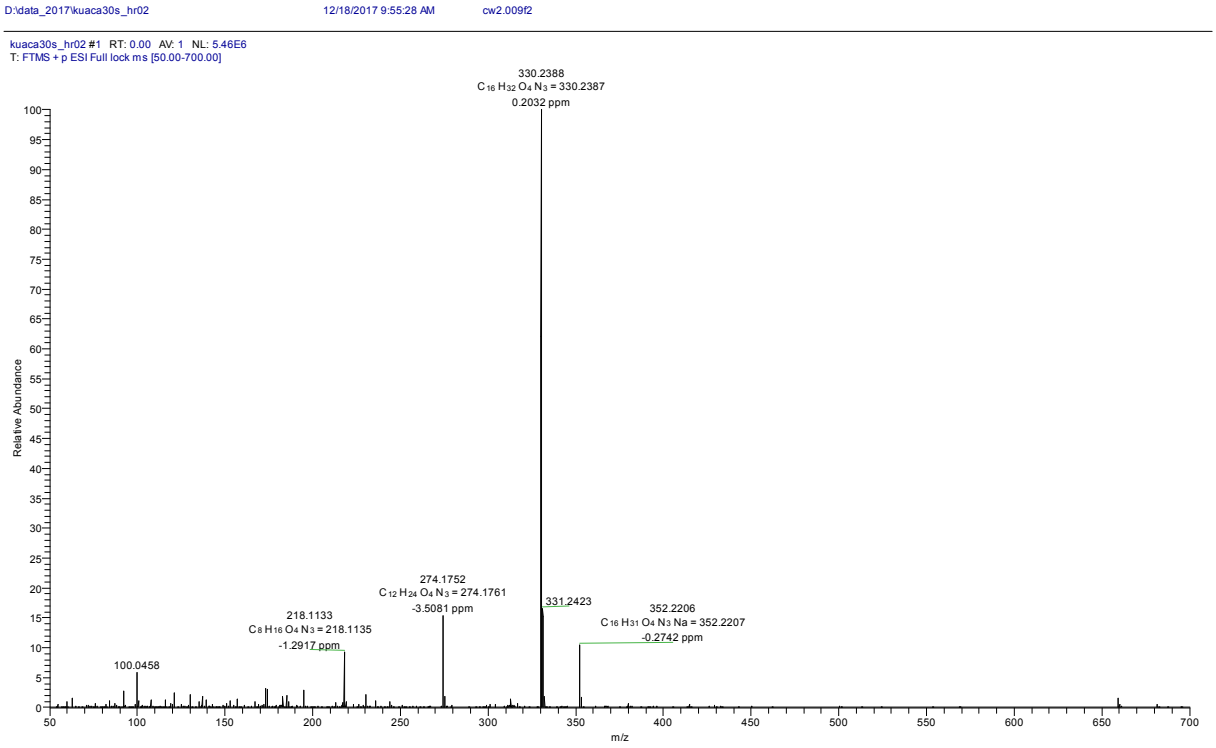

Figure S17. HR-ESI(+) spectrum of di-tert-butyl (1,4,7-triazonane-1,4-diyl) bis(carbonate) (**5**)

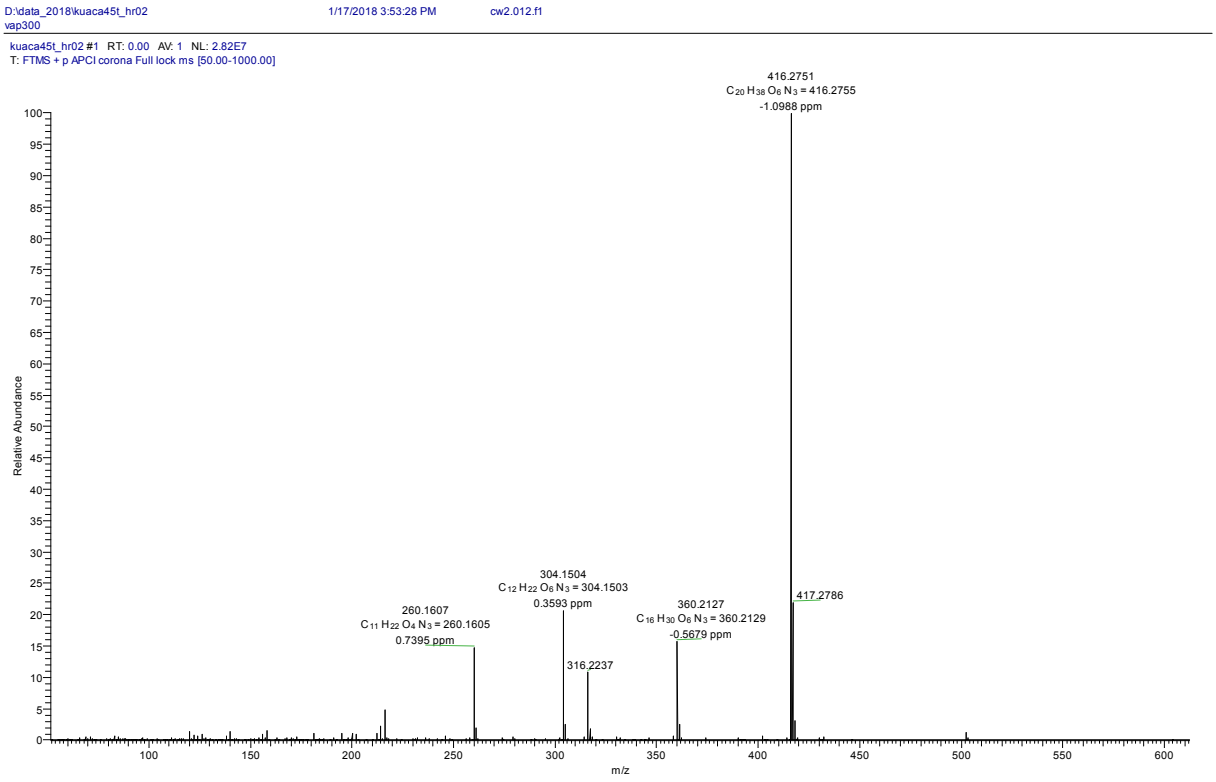

Figure S18. HR-ESI(+) spectrum of ethyl 2-(4,7-bis((tert-butoxycarbonyl)oxy)-1,4,7-triazonan-1-yl)acetate (**6**)

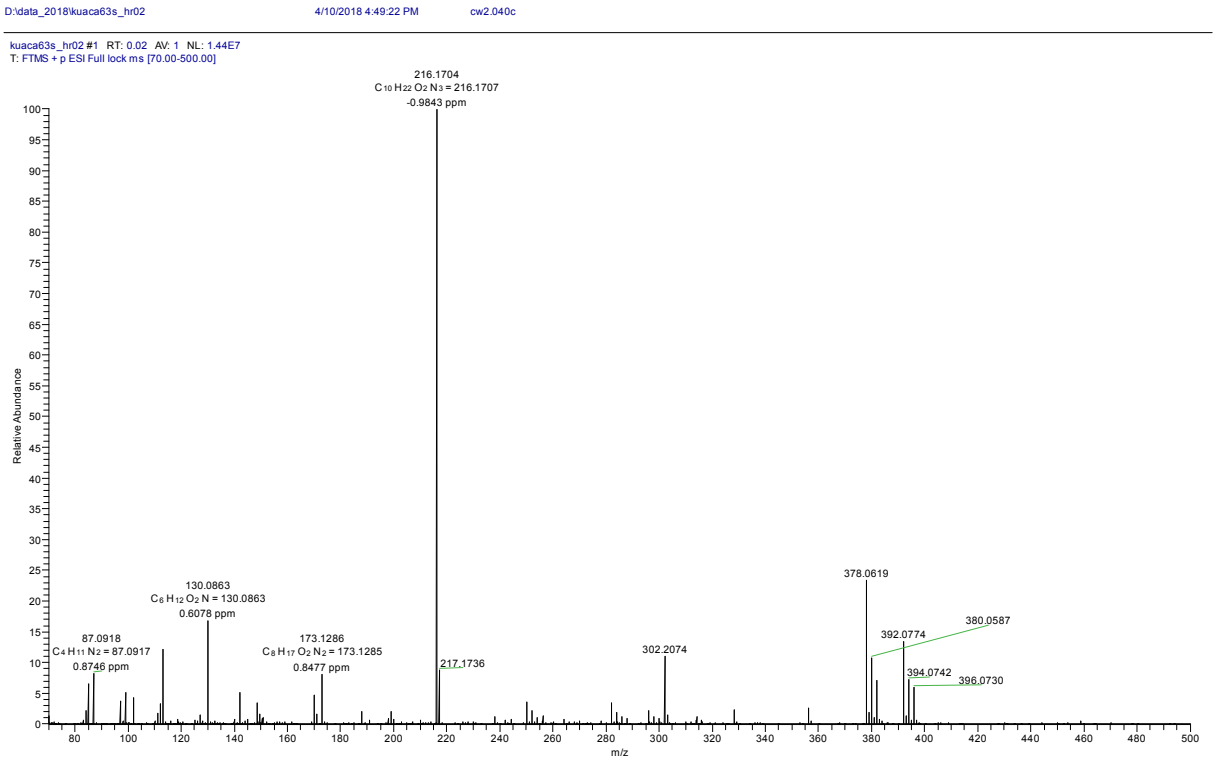

Figure S19. HR-ESI(+) spectrum of ethyl 2-(1,4,7-triazonan-1-yl)acetate (**7**)

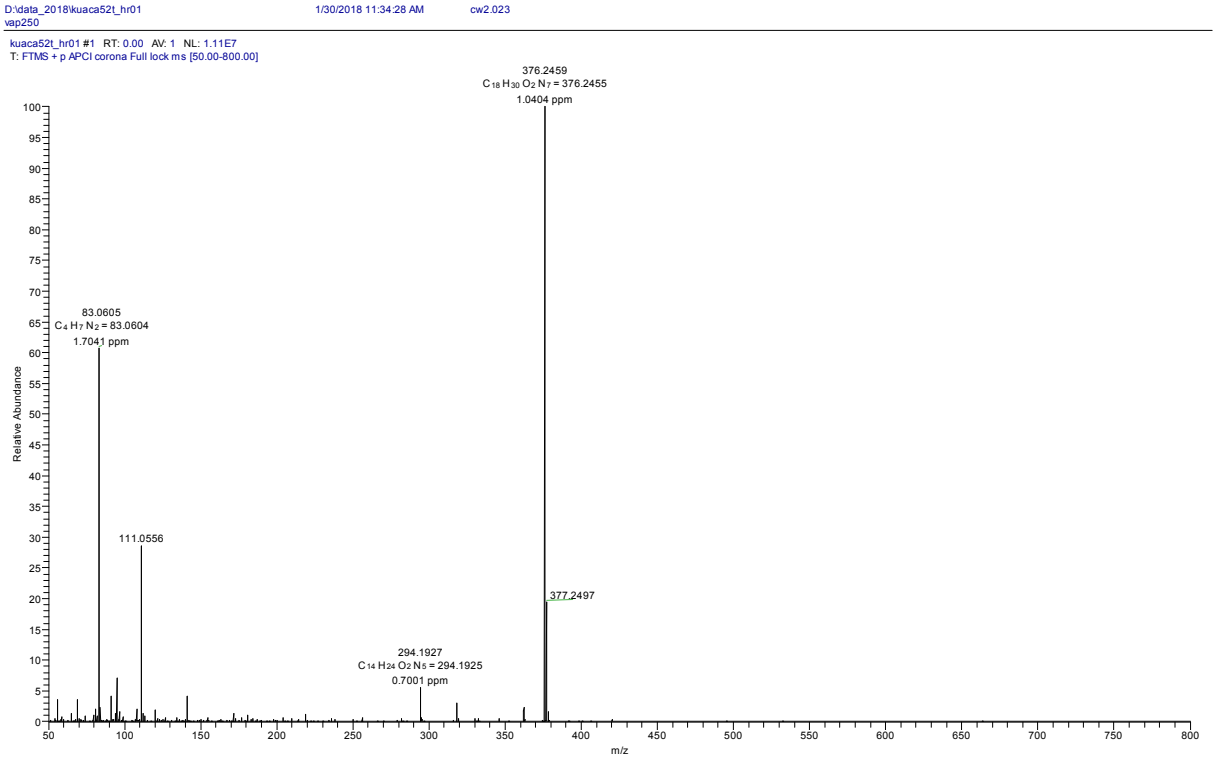

Figure S20. HR-ESI(+) spectrum of 2-(4-((1-Methyl-1H-imidazol-2-yl)methyl)-7-((1-methyl-4,5-dihydro-1H-imidazol-2-yl)methyl)-1,4,7-triazonan-1-yl)acetic acid (NODIA-Me) (**8**)

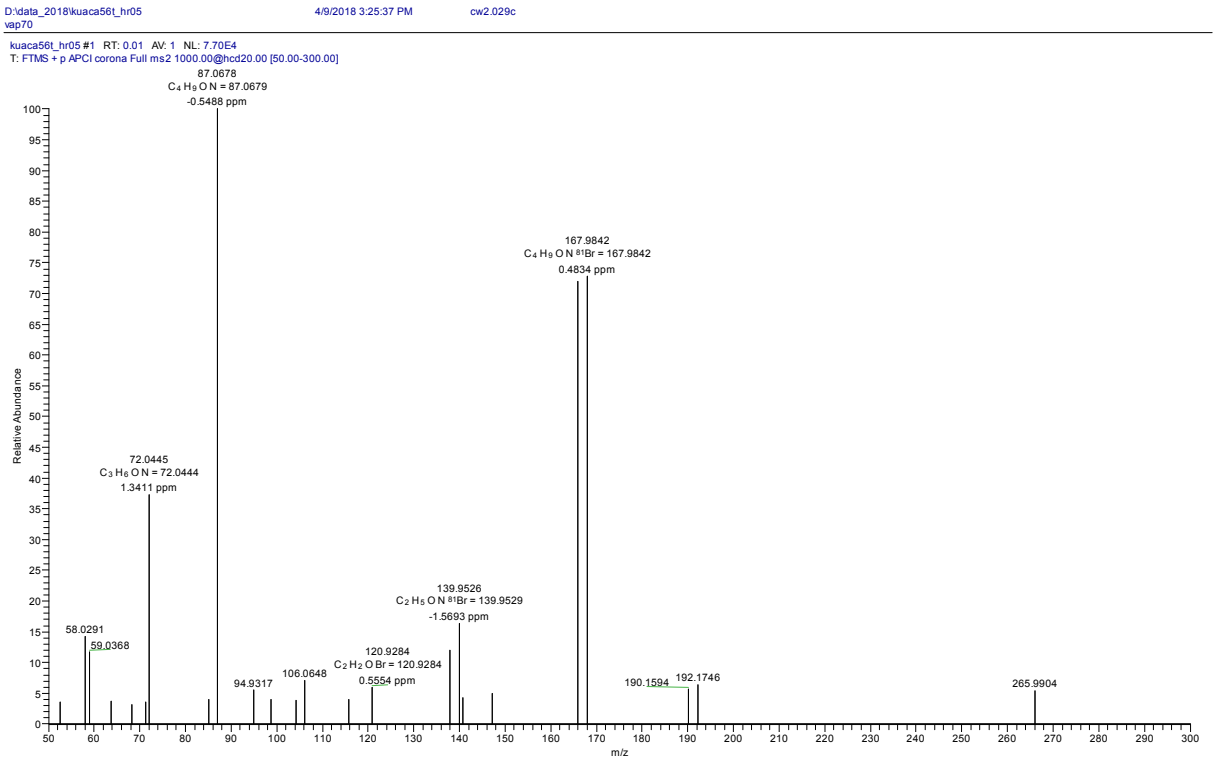

Figure S21. HR-ESI(+) spectrum of 2-bromo-N-ethylacetamide (**9**)

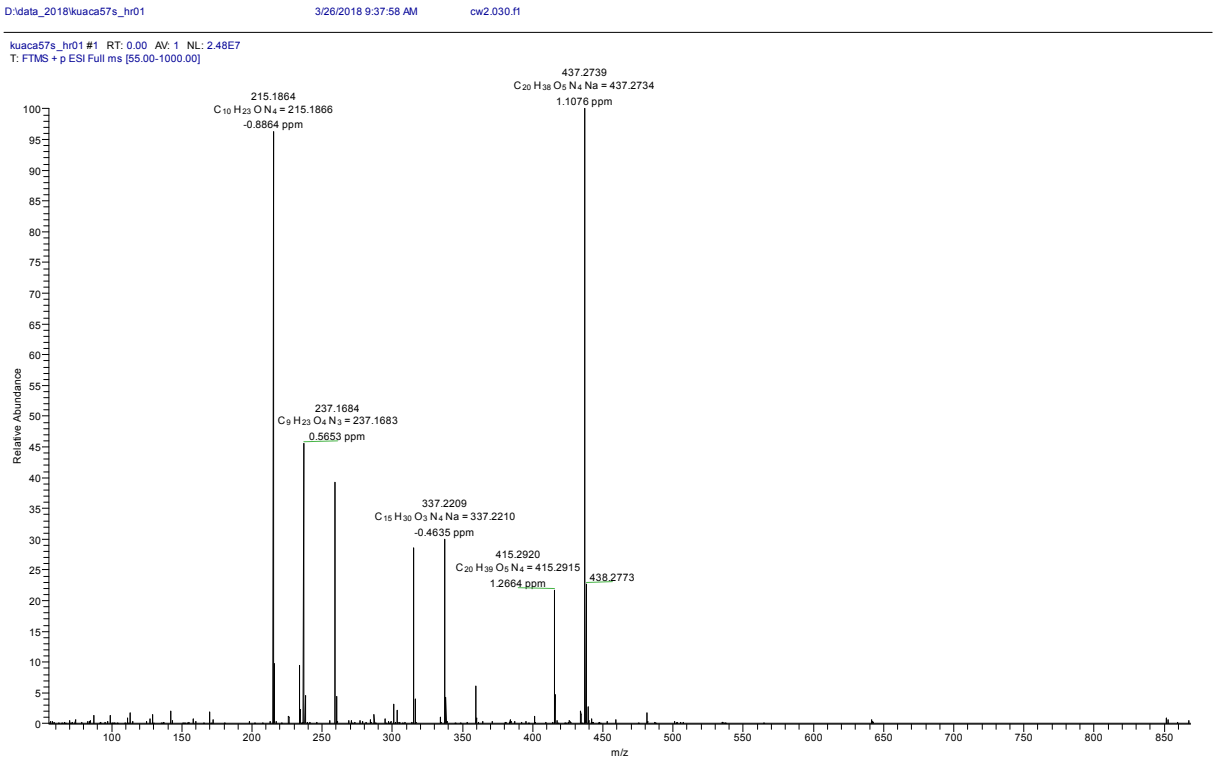

Figure S22. HR-ESI(+) spectrum of di-tert-butyl 7-(2-(ethylamino)-2-oxoethyl)-1,4,7-triazonane-1,4-dicarboxylate (**10**)

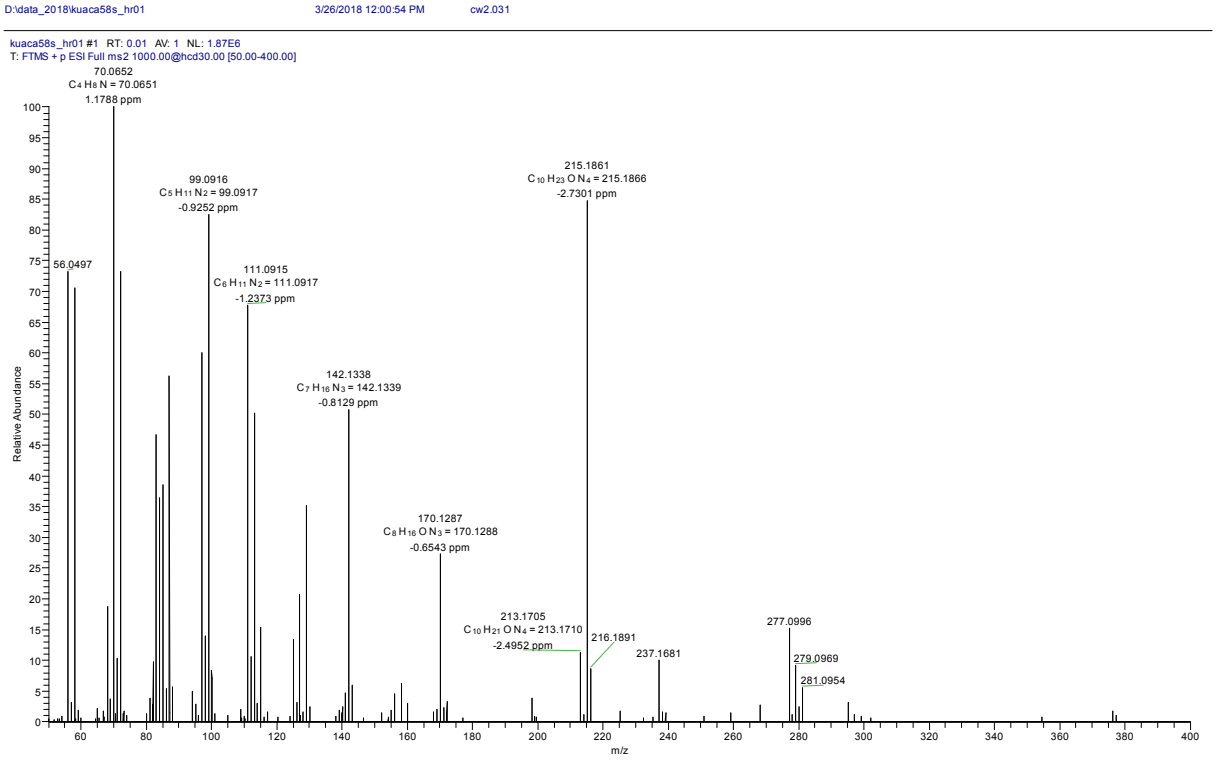

Figure S23. HR-ESI(+) spectrum of N-ethyl-2-(1,4,7-triazonan-1-yl)acetamide (**11**)

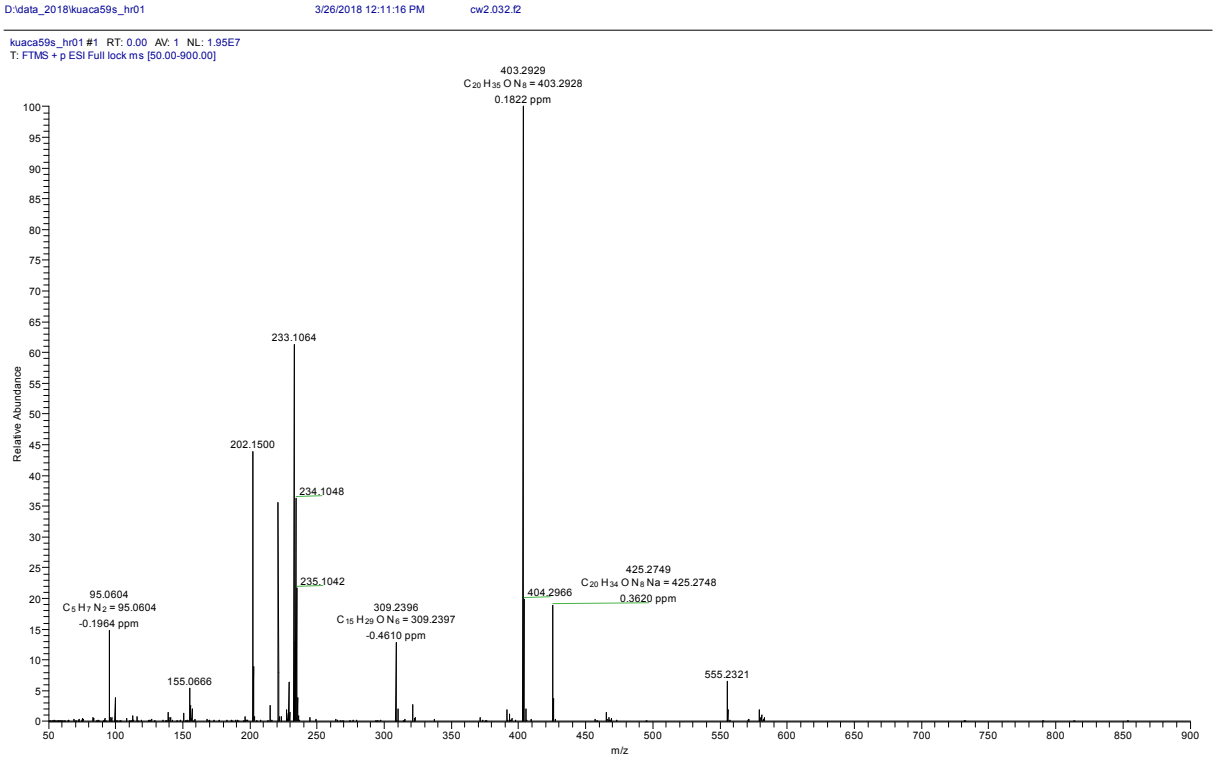

Figure S24. HR-ESI(+) spectrum of 2-(4,7-Bis((1-methyl-1H-imidazol-2-yl)methyl)-1,4,7-triazonan-1-yl)-N-ethylacetamide NODIA-Me-NH-Et (**12**)

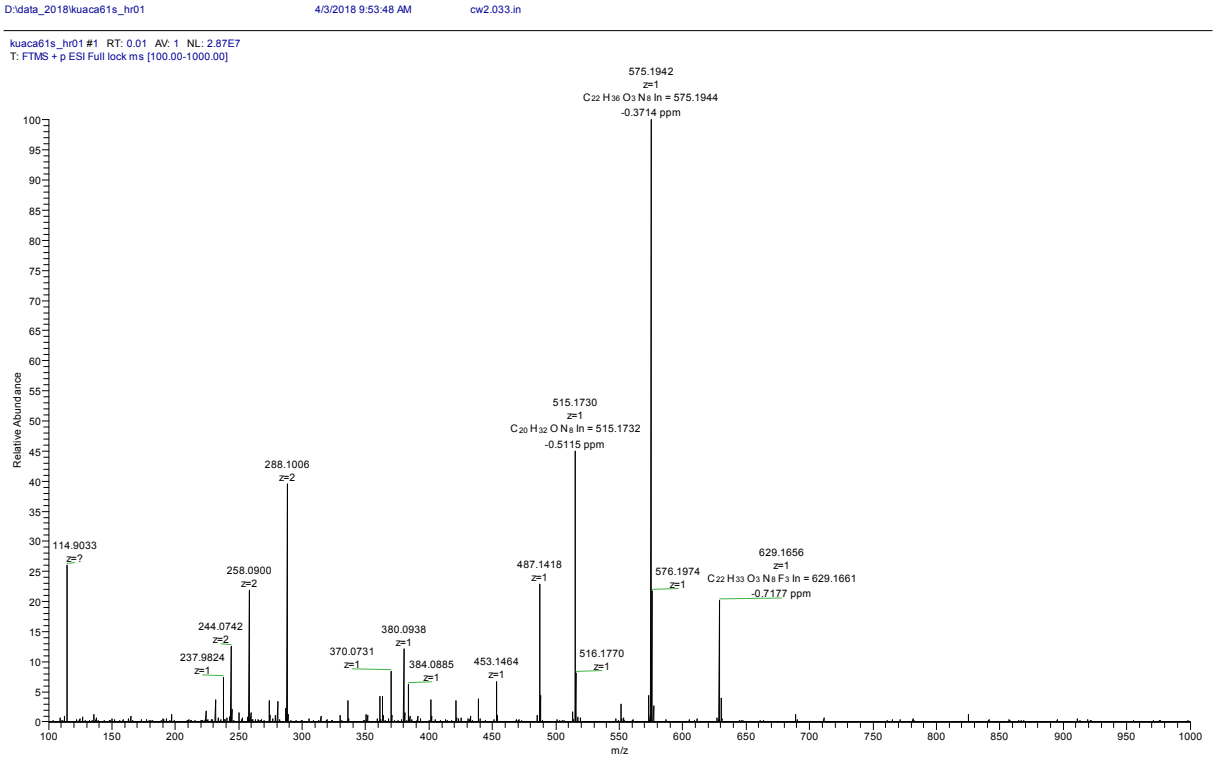

Figure S25. HR-ESI(+) spectrum of In-**12**

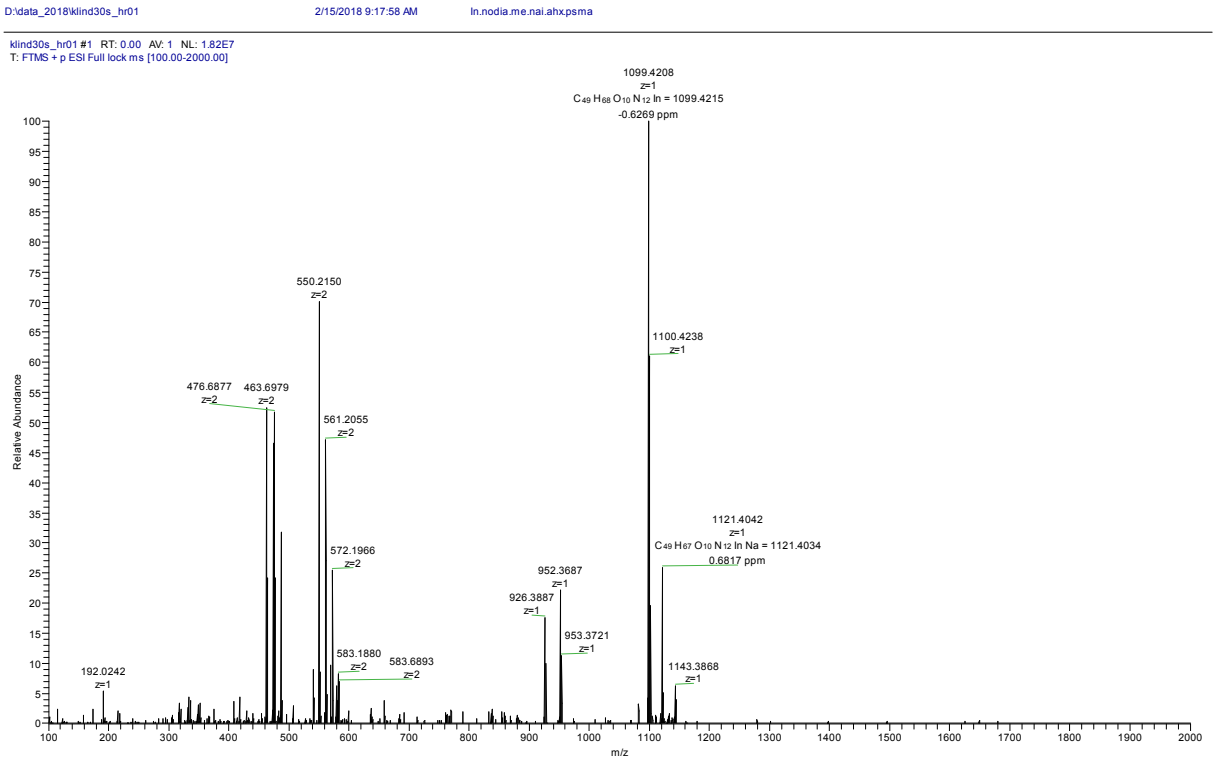

Figure S26. HR-ESI(+) spectrum of In-**13**

HPLC characterization

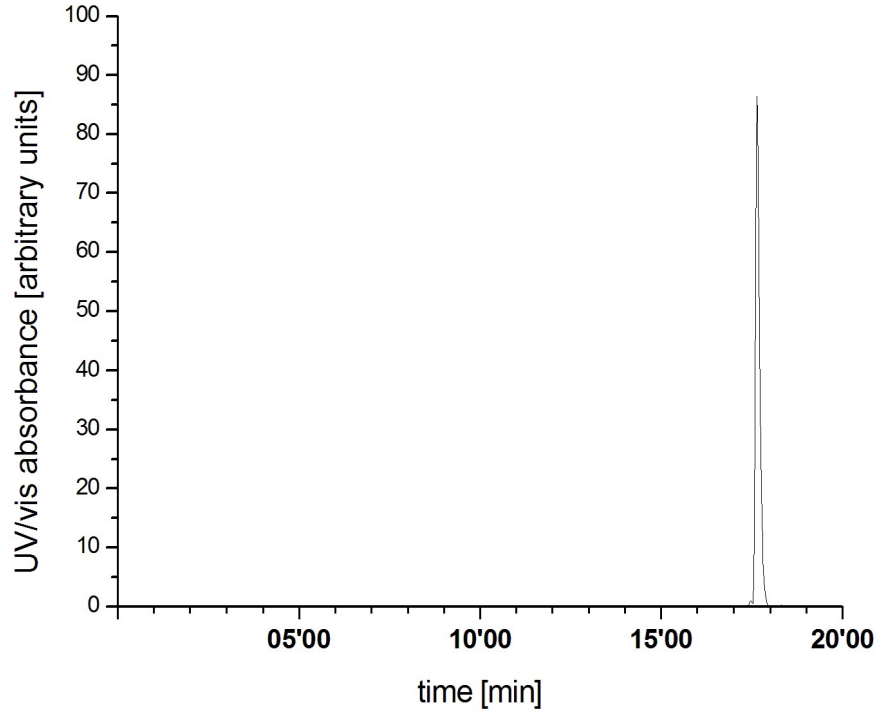

Figure S27. UV trace of ^{nat}In-**13**

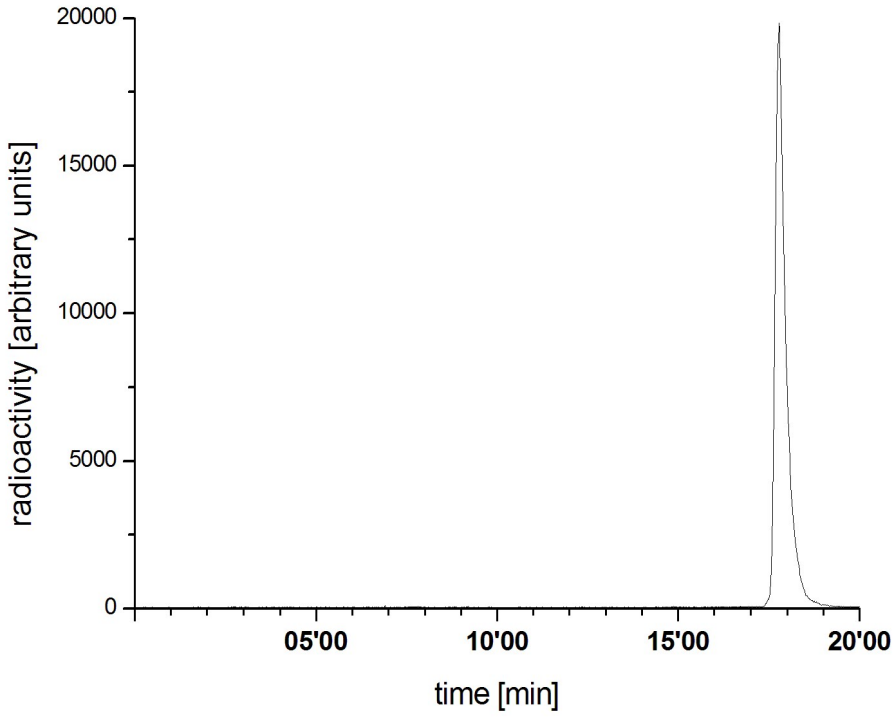

Figure S28. Radioactivity trace of [^{111}In]In-**13** after incubation in DTPA after 24 h

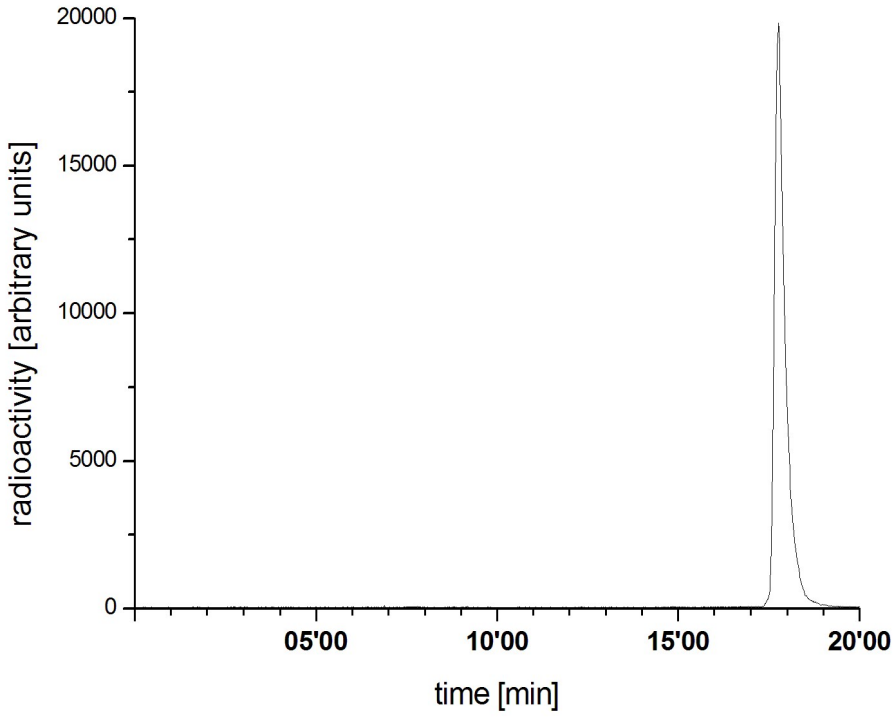

Figure S29. Radioactivity trace of [^{111}In]In-**13** after incubation in human serum after 24 h

IR measurements

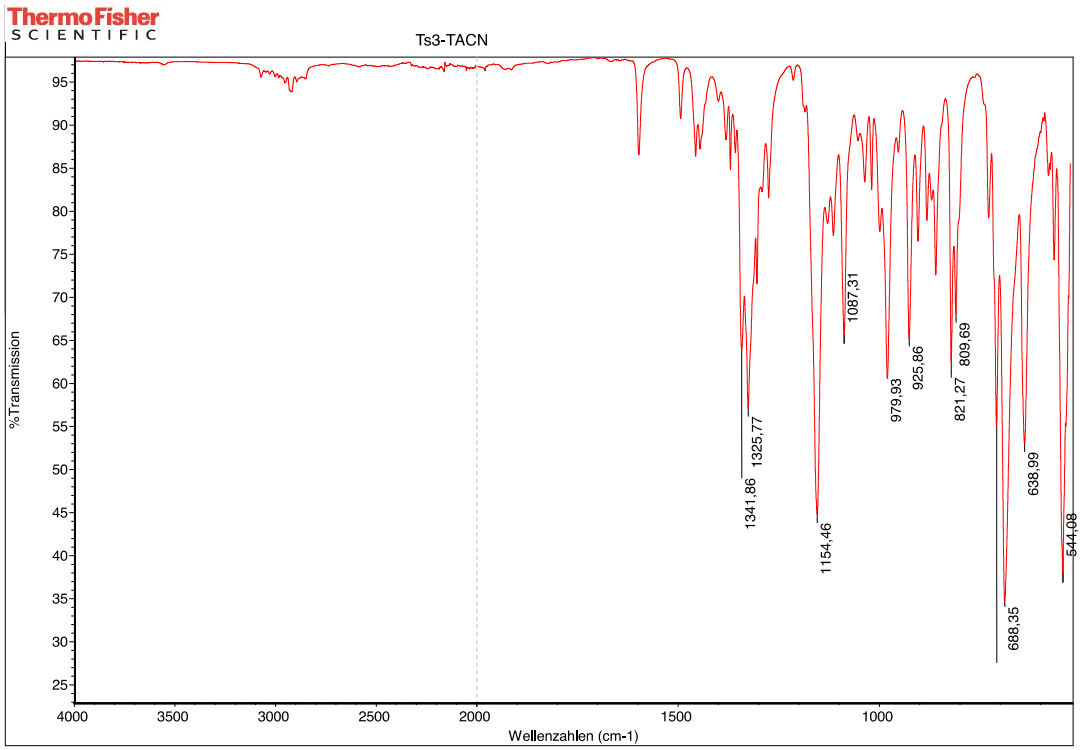

Figure S30. IR spectrum of **1**

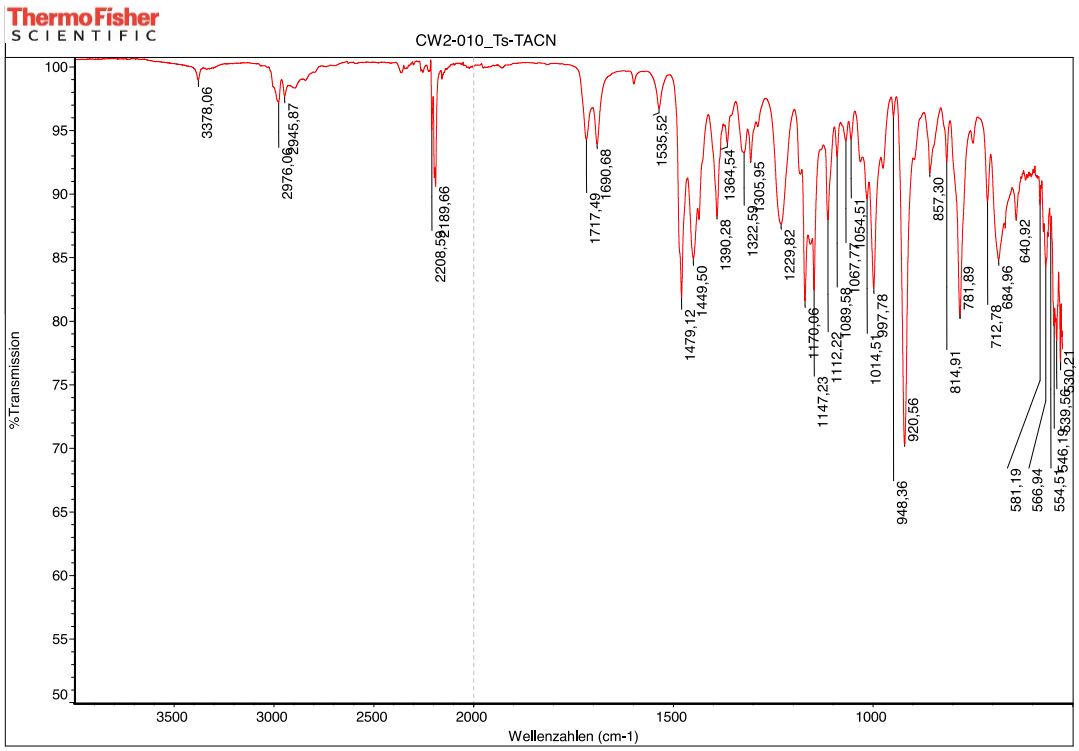

Figure S31. IR spectrum of **2**

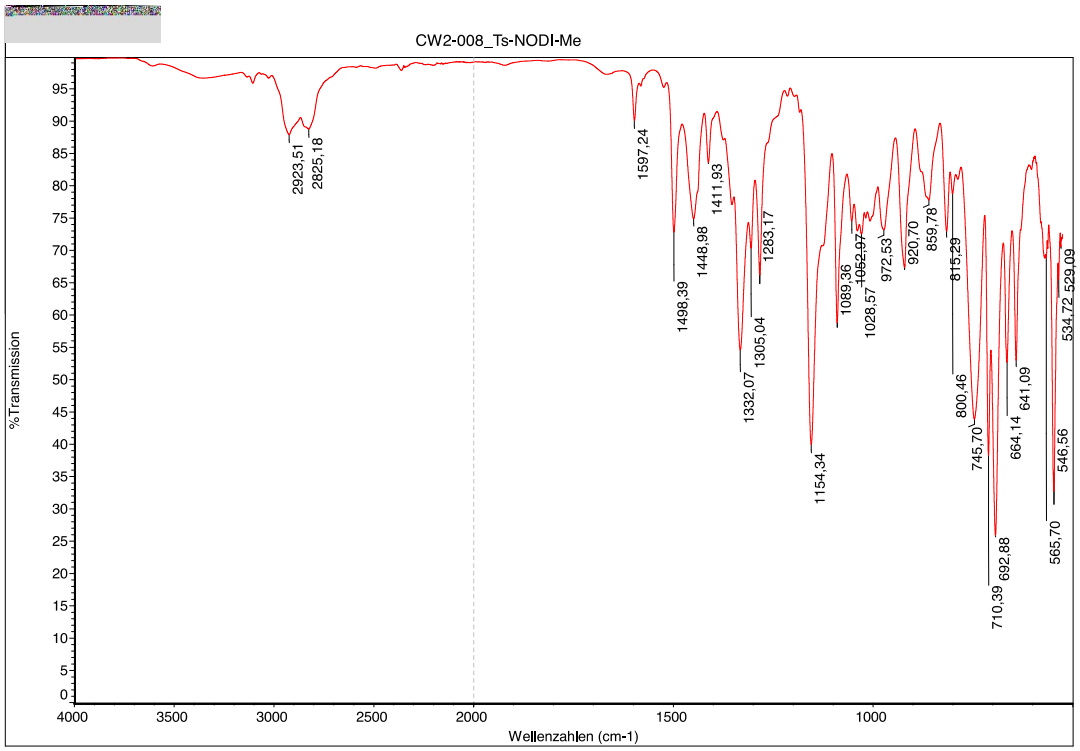

Figure S32. IR spectrum of **3**

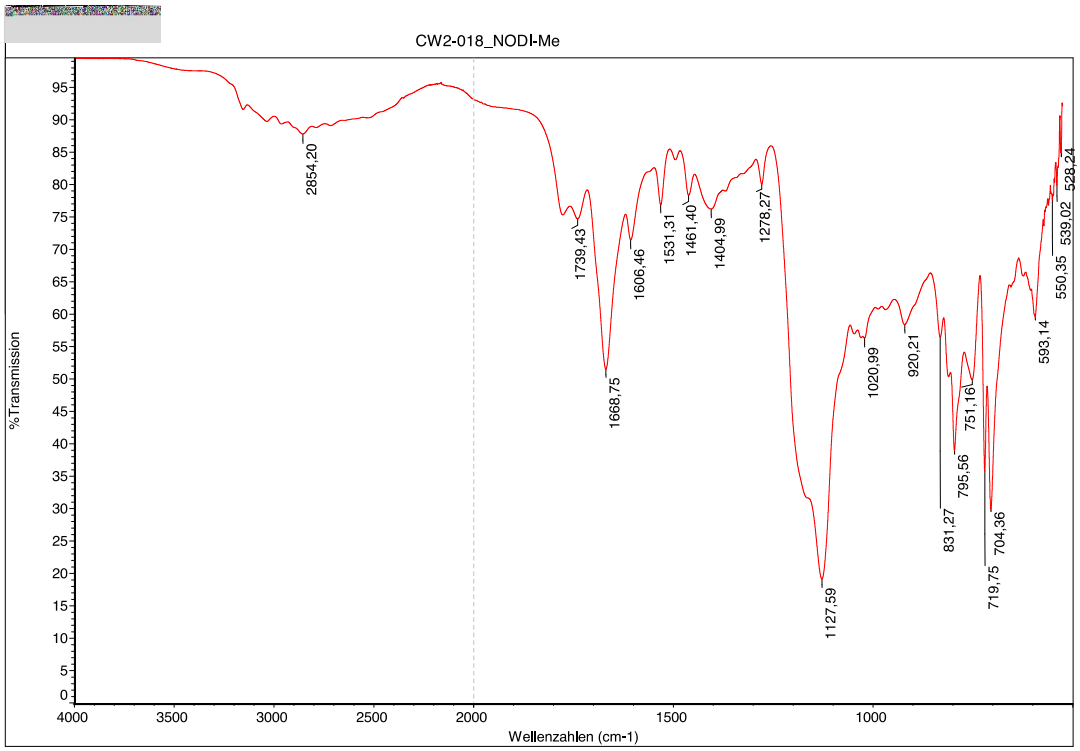

Figure S33. IR spectrum of **4**

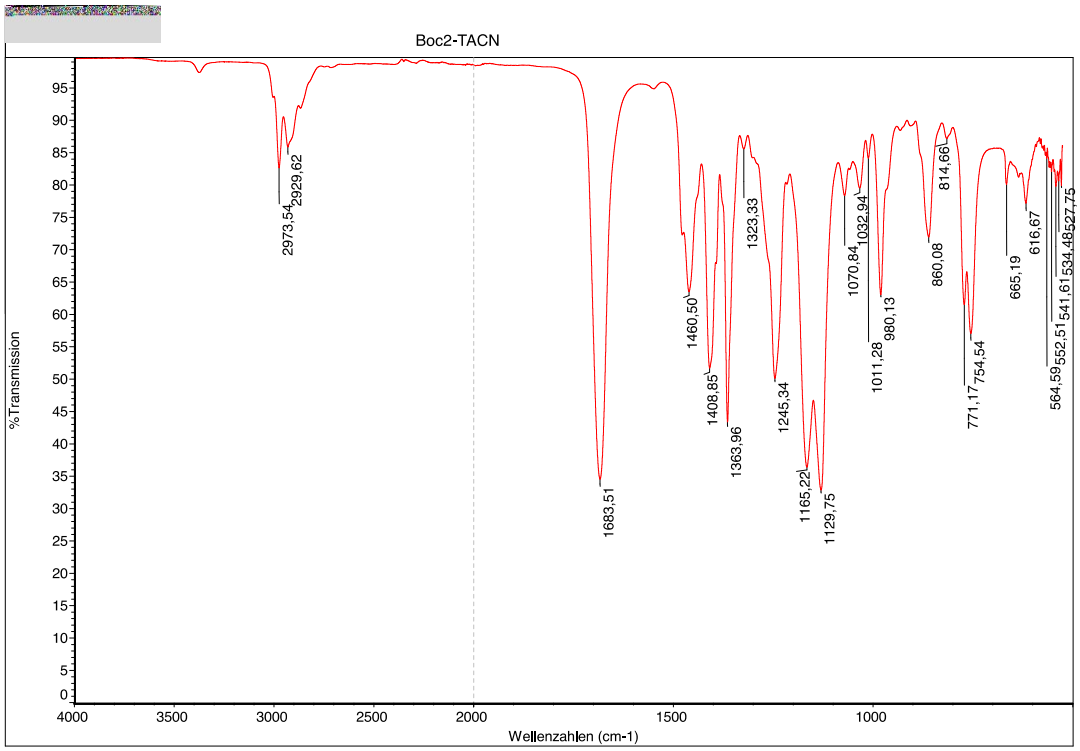

Figure 34. IR spectrum of **5**

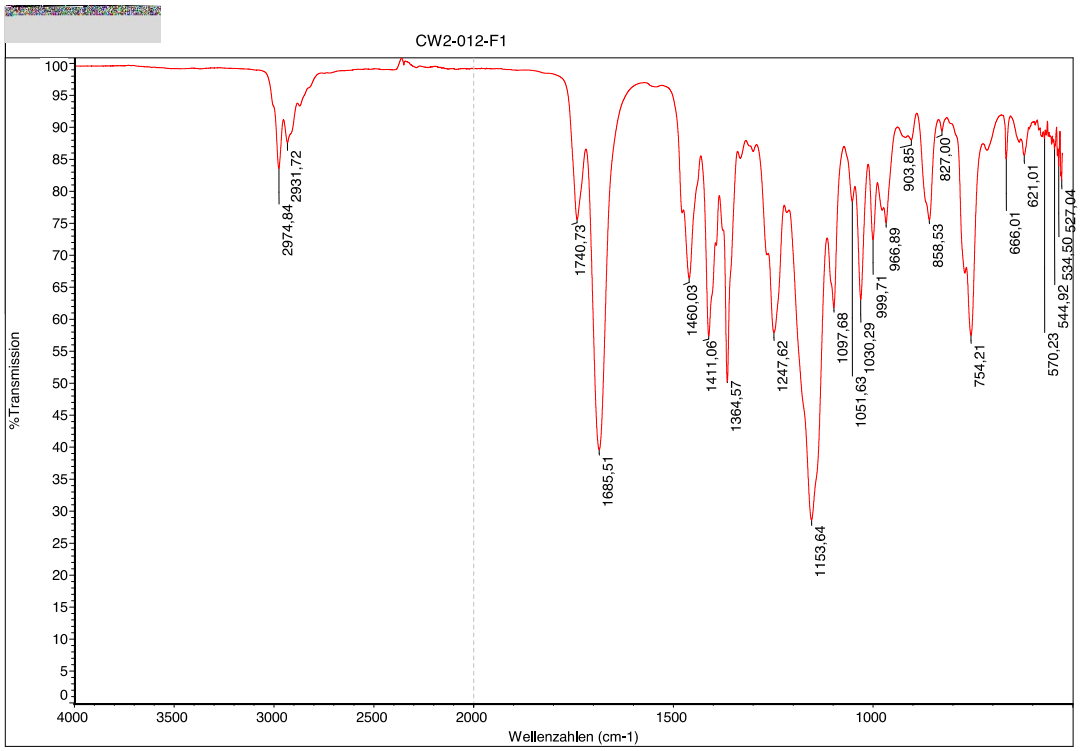

Figure S35. IR spectrum of **6**

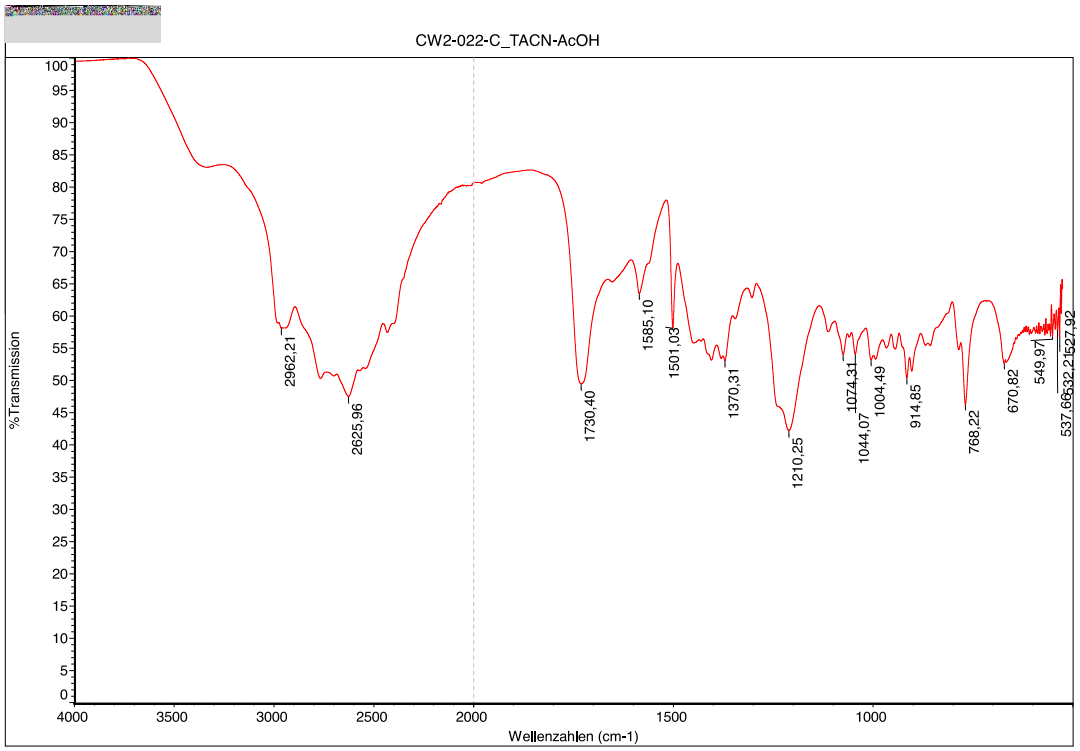

Figure S36. IR spectrum of **7**

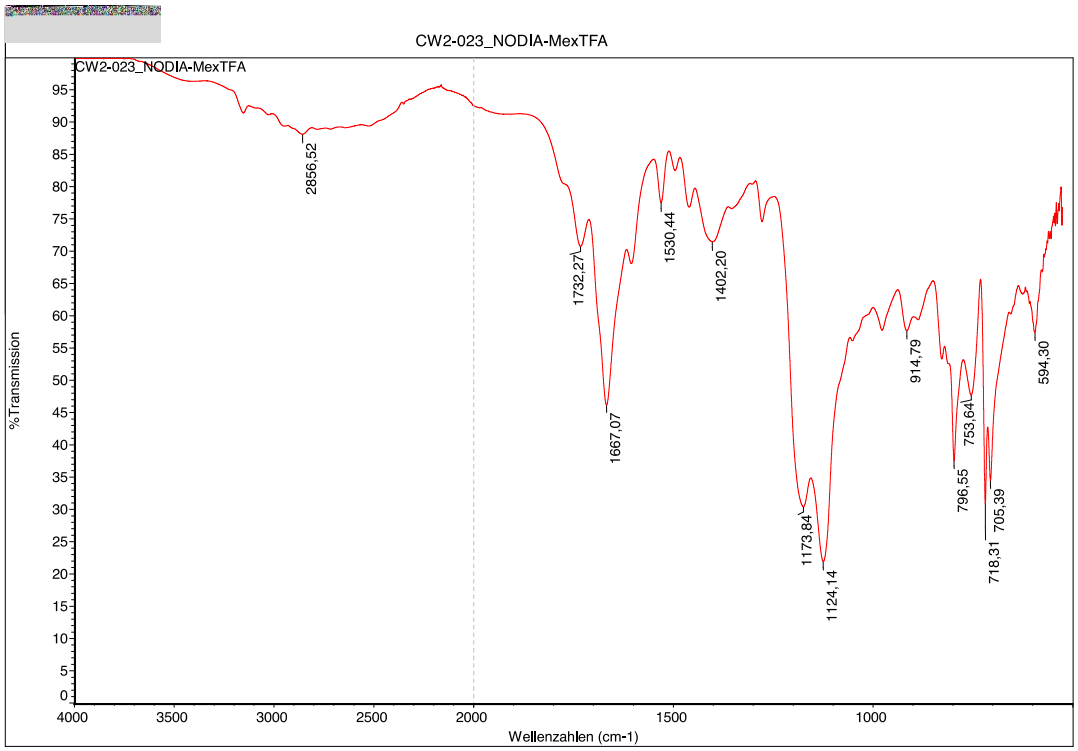

Figure S37. IR spectrum of **8**

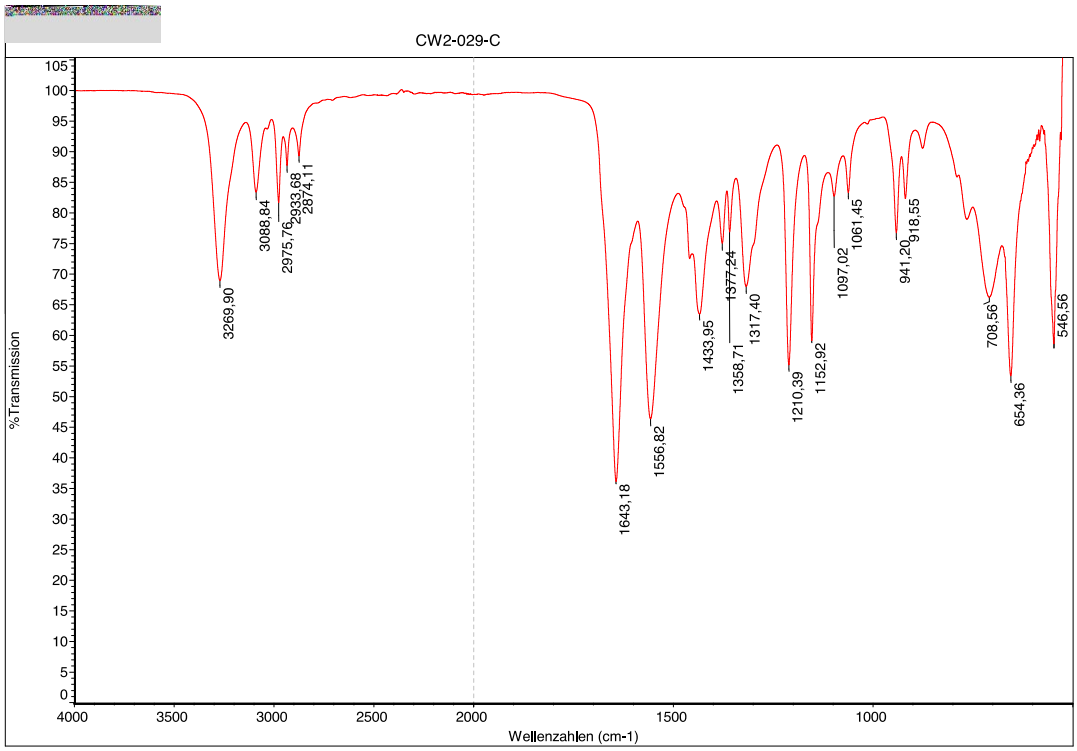

Figure S38. IR spectrum of **9**

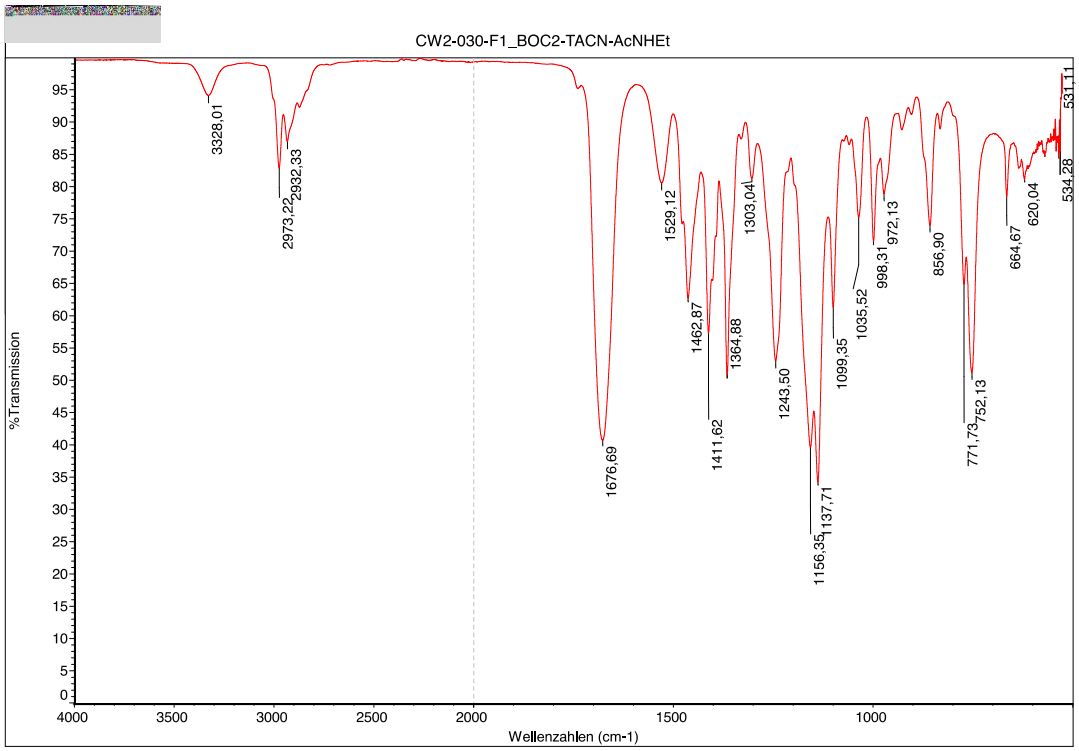

Figure S39. IR spectrum of **10**

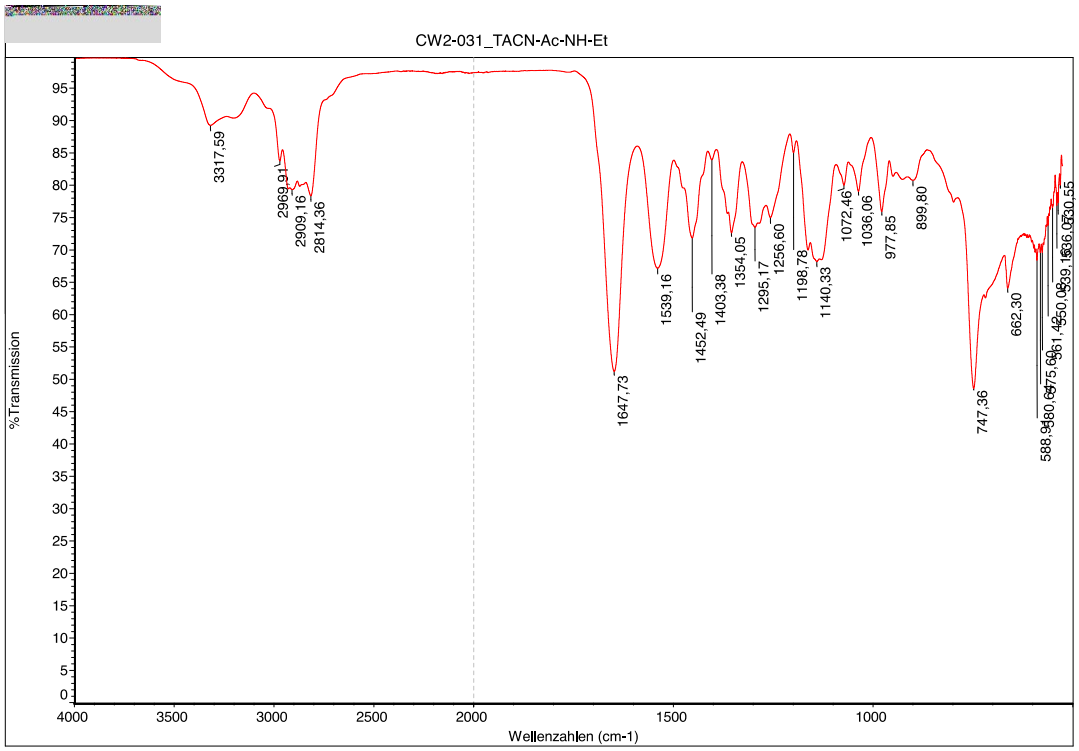

Figure S40. IR spectrum of **11**

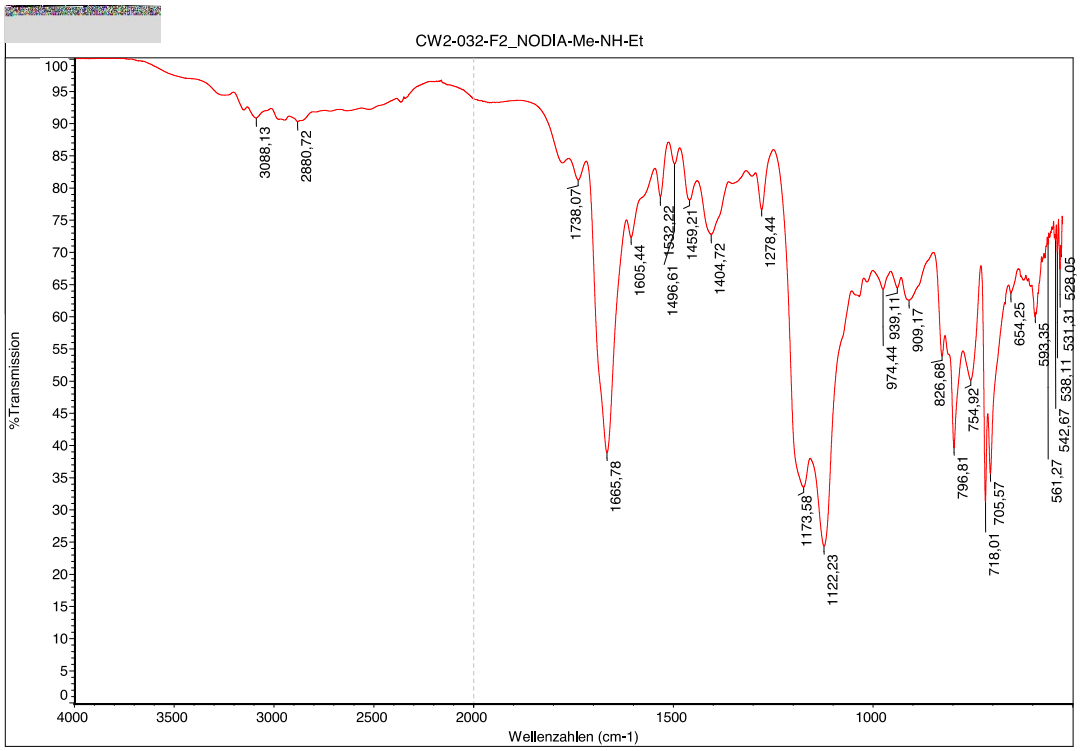

Figure S41. IR spectrum of **12**

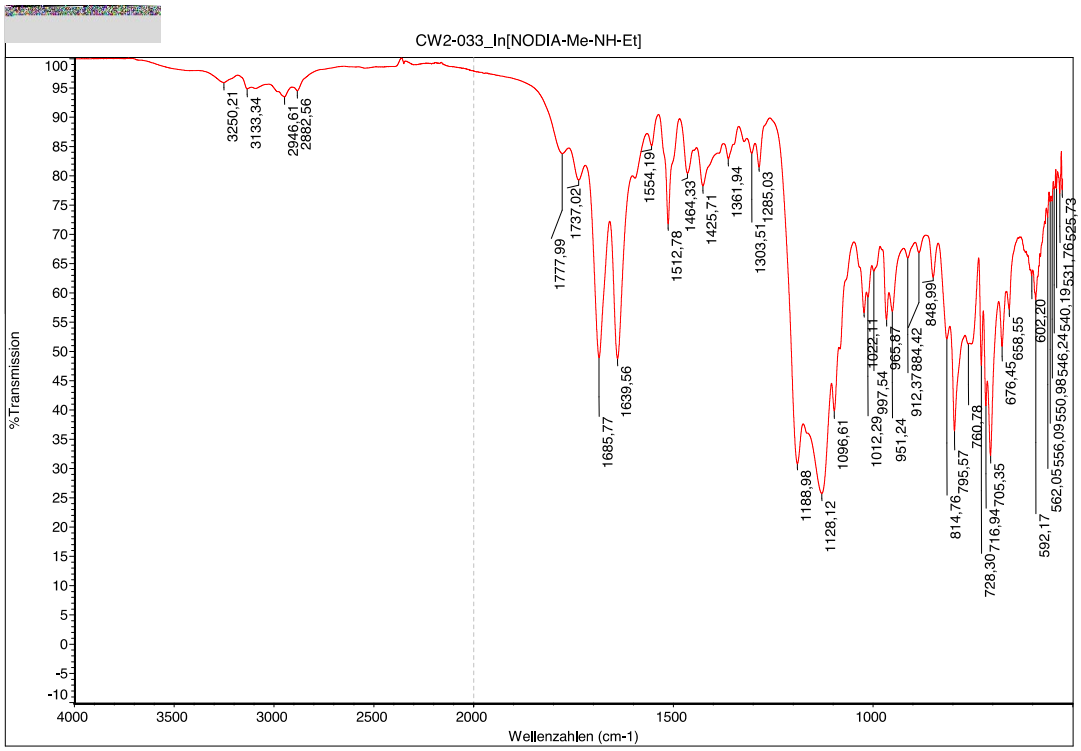

Figure S42. IR spectrum of In-**12**